RUHR-UNIVERSITÄT BOCHUM

The FlareLab-Experiment:

Laboratory Simulation of Arched Solar Prominences

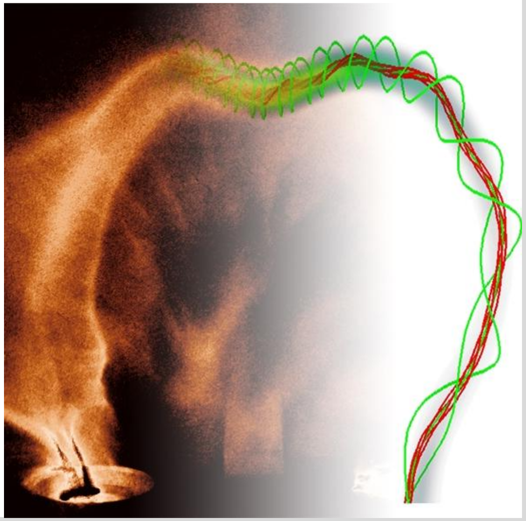

Henning Soltwisch

AG Laser- und Plasmaphysik

FlareLab:

collaborative effort between laboratory investigations and numerical simulations of structures similar to solar prominences

Felix Mackel
Sascha Ridder
Jan Tenfelde
Philipp Kempkes[a)]
Henning Soltwisch

Institut für Experimentalphysik

AG Laser- und Plasmaphysik und

[a)] MPI and University Greifswald, Germany

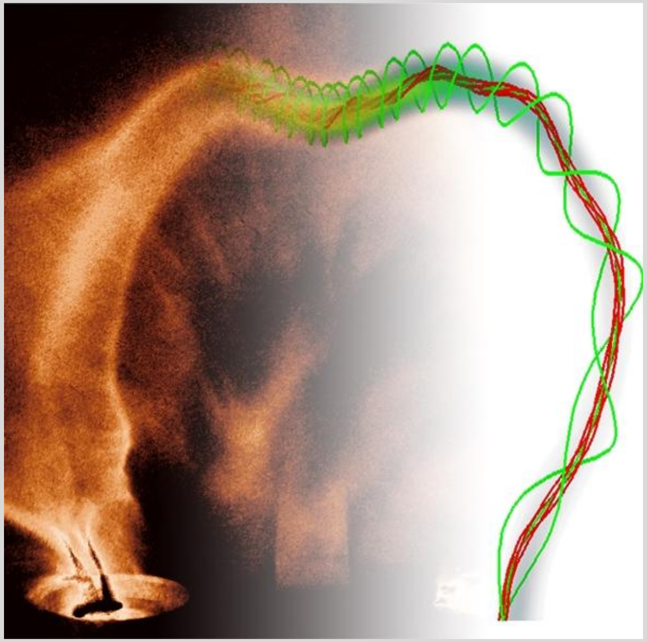

Thomas Tacke
Jürgen Dreher
Rainer Grauer

Institut für Theoretische Physik

Lehrstuhl für Plasma-, Laser- und Atomphysik

The FlareLab-Experiment: Introduction

PHYSICS OF PLASMAS VOLUME 5, NUMBER 5 MAY 1998

Laboratory simulations of solar prominence eruptions*

P. M. Bellan† and J. F. Hansen
California Institute of Technology, Pasadena, California 91125

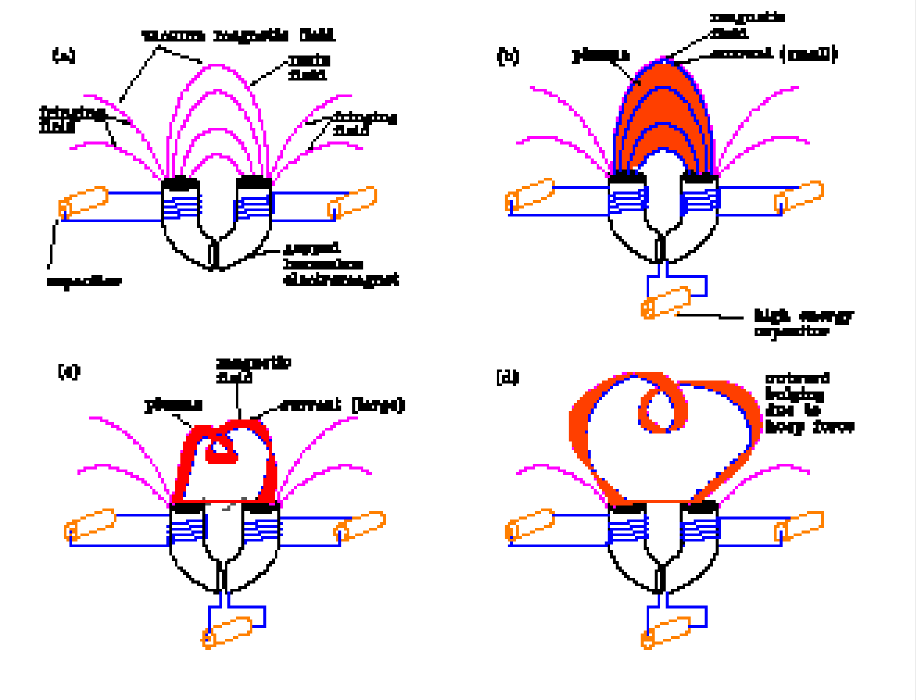

The FlareLab-Experiment: Principle of operation

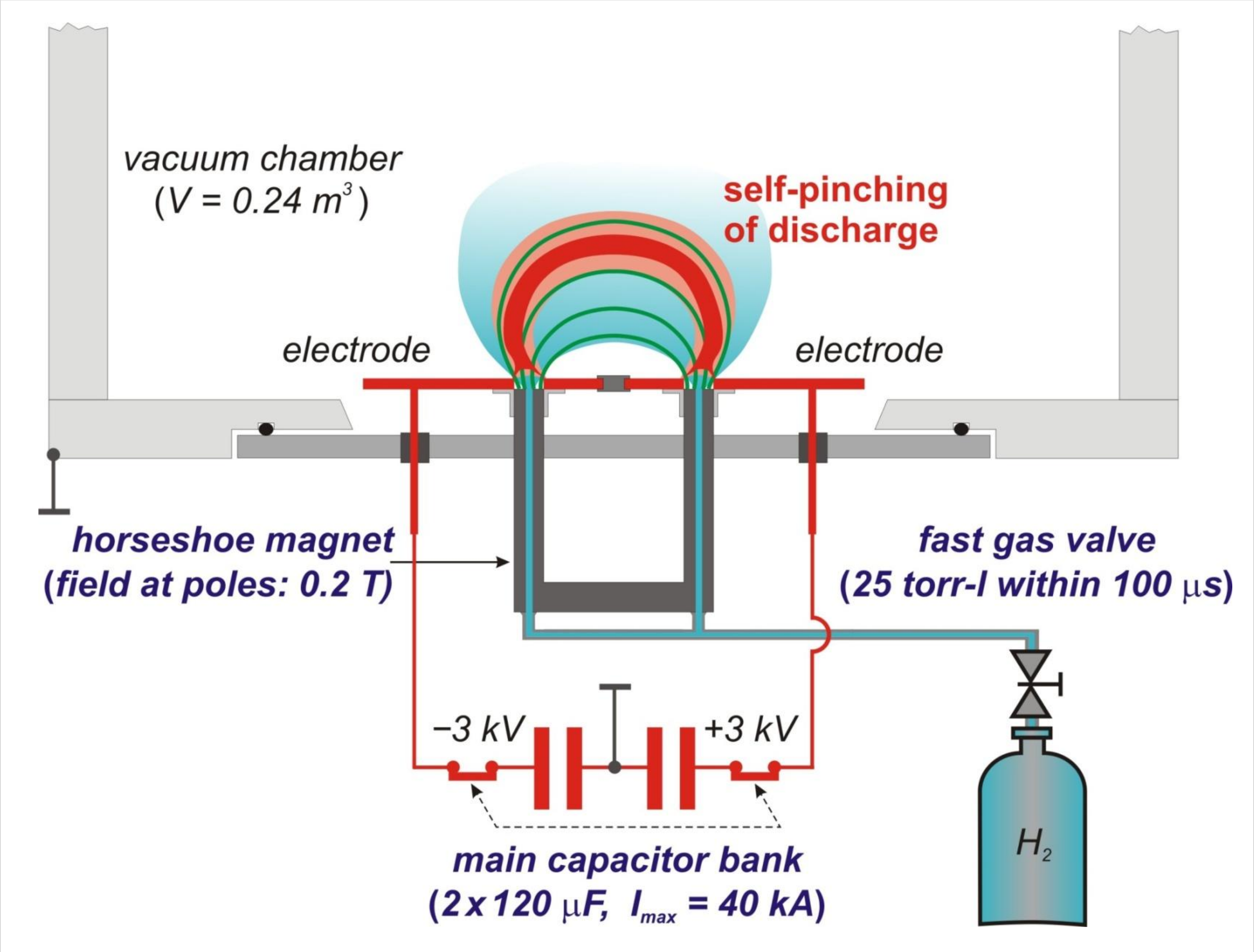

The FlareLab-Experiment: Technical design and construction

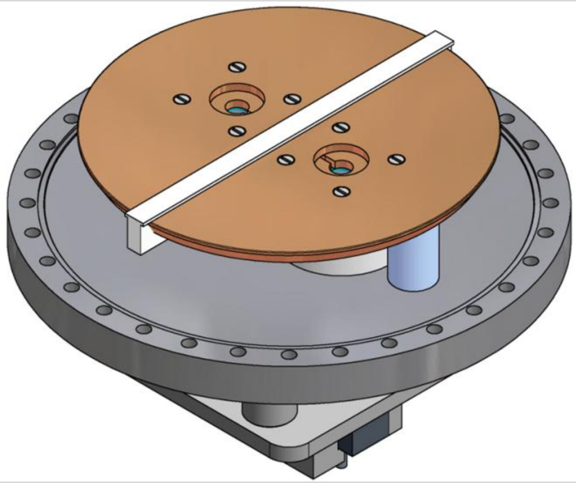

electrodes, gas inlet,
horseshoe magnet

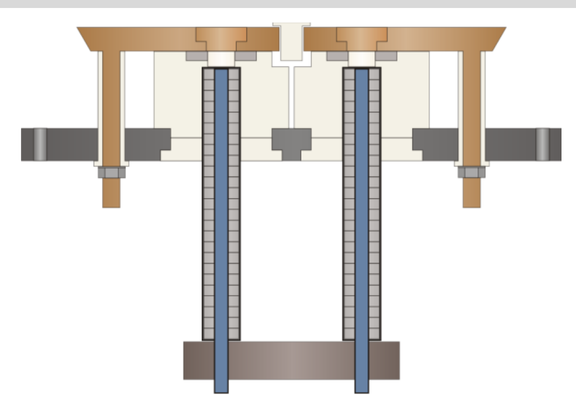

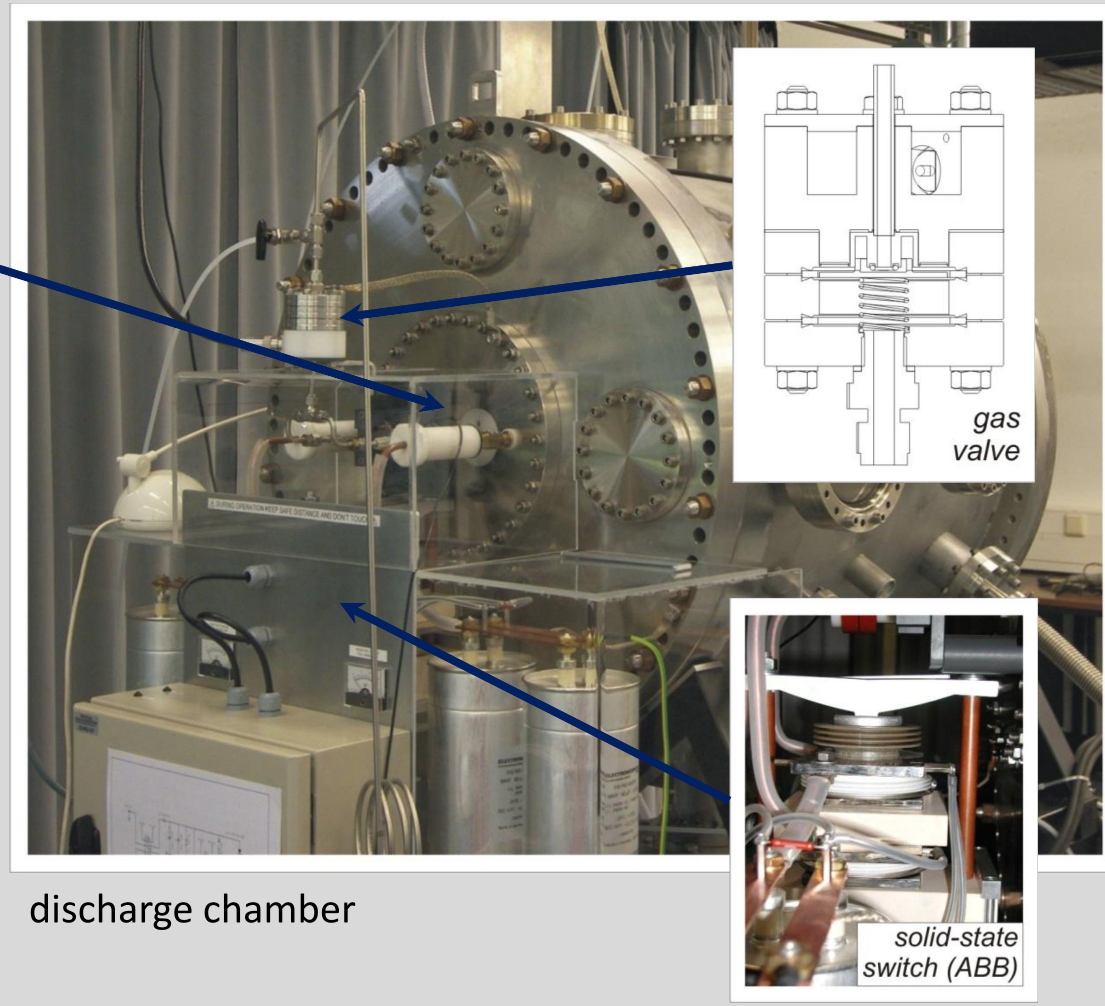

discharge chamber

The FlareLab-Experiment: Temporal evolution of a discharge

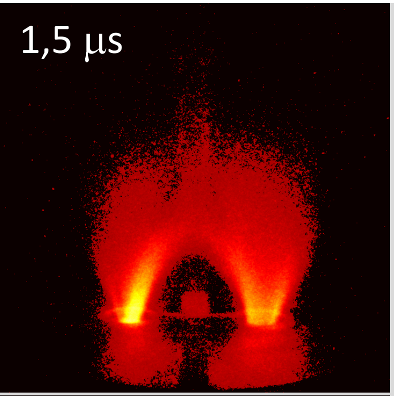

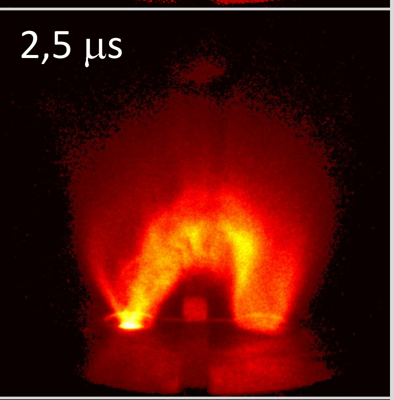

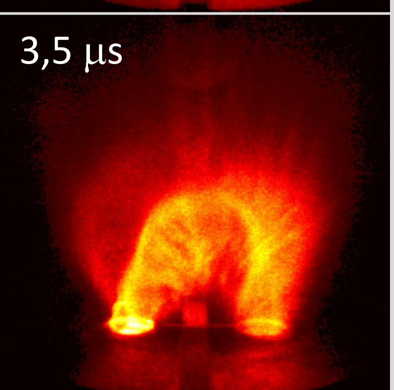

discharge current **(blue)** and
voltage at neg. electrode **(red)**

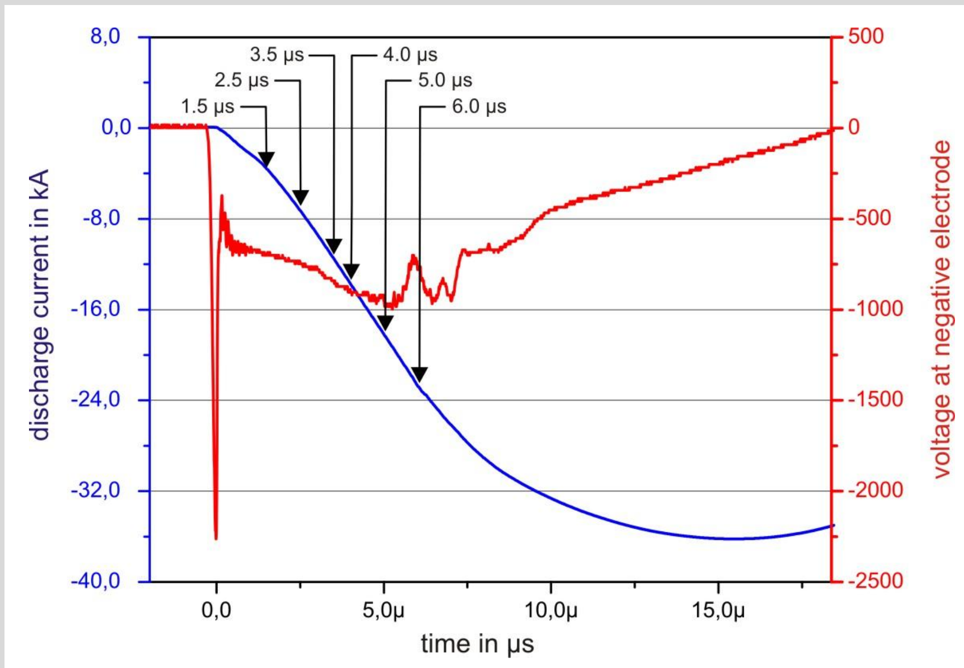

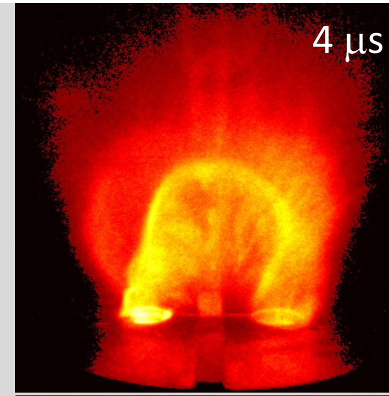

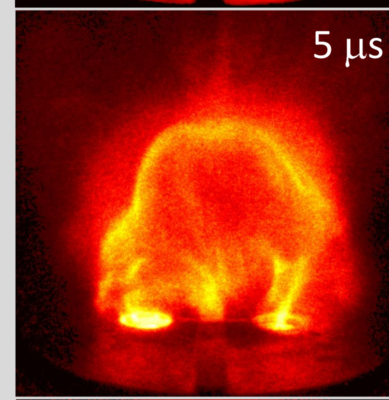

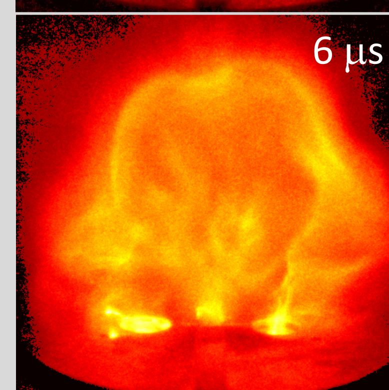

(exposure times: 50 ns)

The FlareLab-Experiment: Diagnostic equipment

- **intensified CCD camera**
  (discharge structure and dynamics)
- **HV probes and Rogowski coils**
  (voltage and current measurements)
- **B-dot probes**
  (local magnetic field measurements)
- **electrostatic triple probes**
  (local measurements of n_e and T_e)
- **standard spectroscopy (visible)**
  (plasma composition; line broadening)
- **XUV diode (metal filter foils)**
  (generation of radiation by fast particles)
- **CO_2 laser interferometer**
  (movable probe beam; line-averaged n_e)

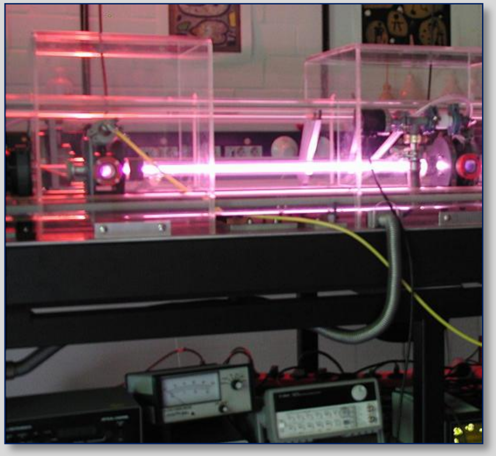

The FlareLab-Experiment: Measurement of plasma parameters (I)

➢ **spectroscopic observations** $\rightarrow$ plasma composition and spatial structure, n_e via Stark broadening

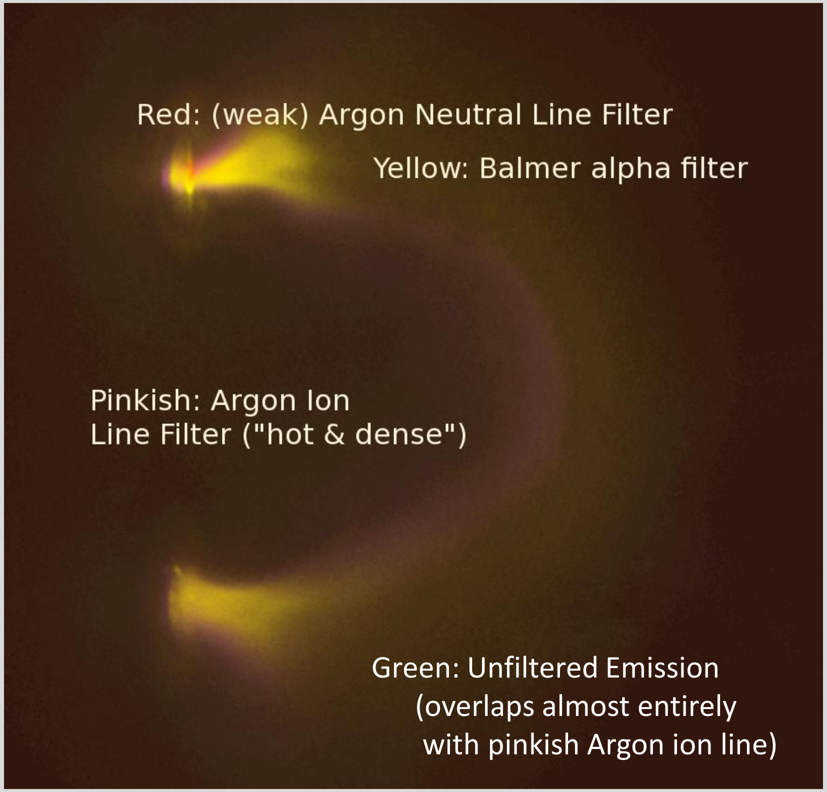

Superposition of discharge images using narrow-band optical filters

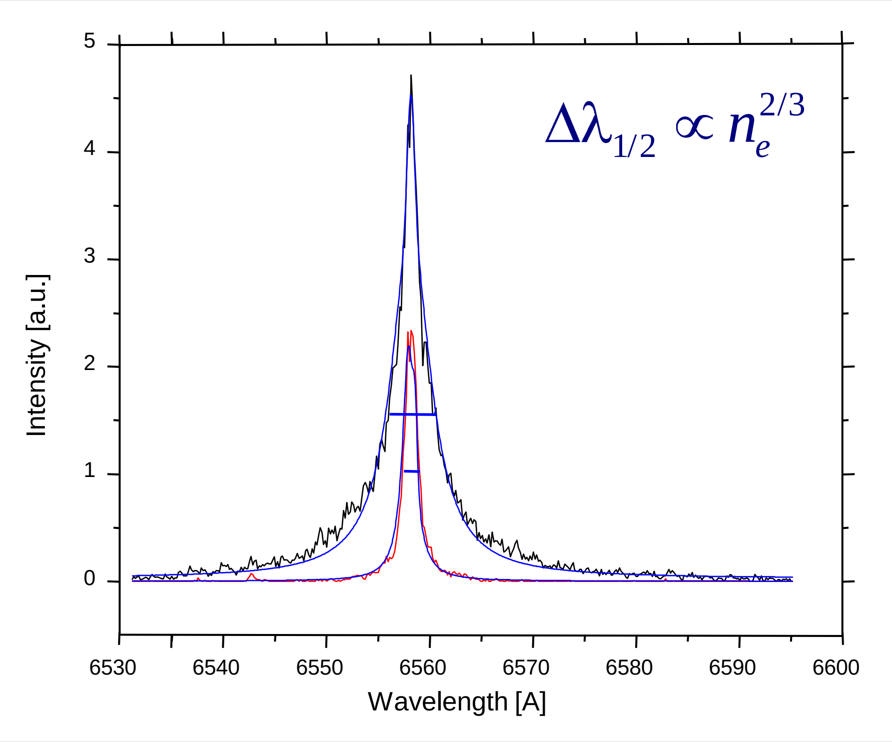

Hydrogen H_α line profiles emitted from plasmas of different electron densities

The FlareLab-Experiment: Measurement of plasma parameters (II)

- **movable electrostatic triple probe** $\rightarrow n_e, T_e$

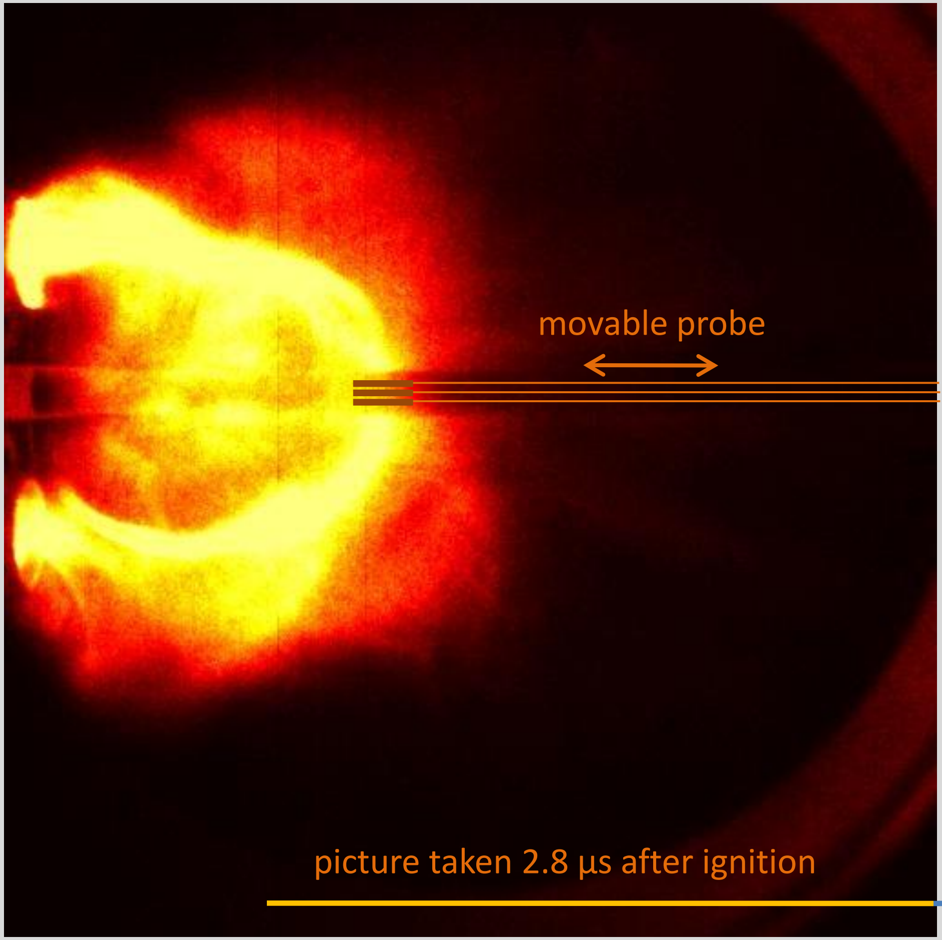

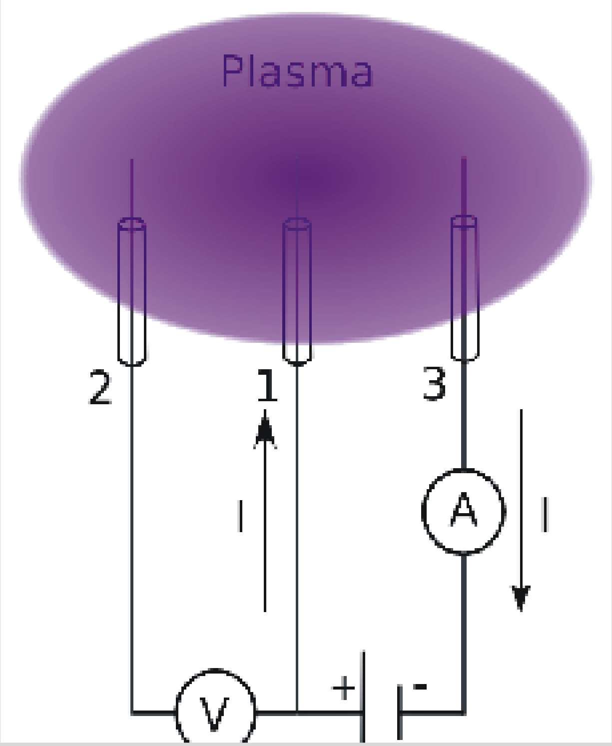

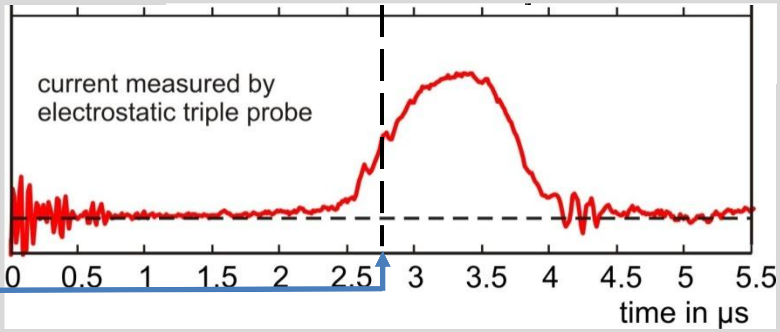

The FlareLab-Experiment: Measurement of plasma parameters (III)

- **movable magnetic pick-up coils exploiting Faraday's law** $\rightarrow B_\theta , B_\varphi$

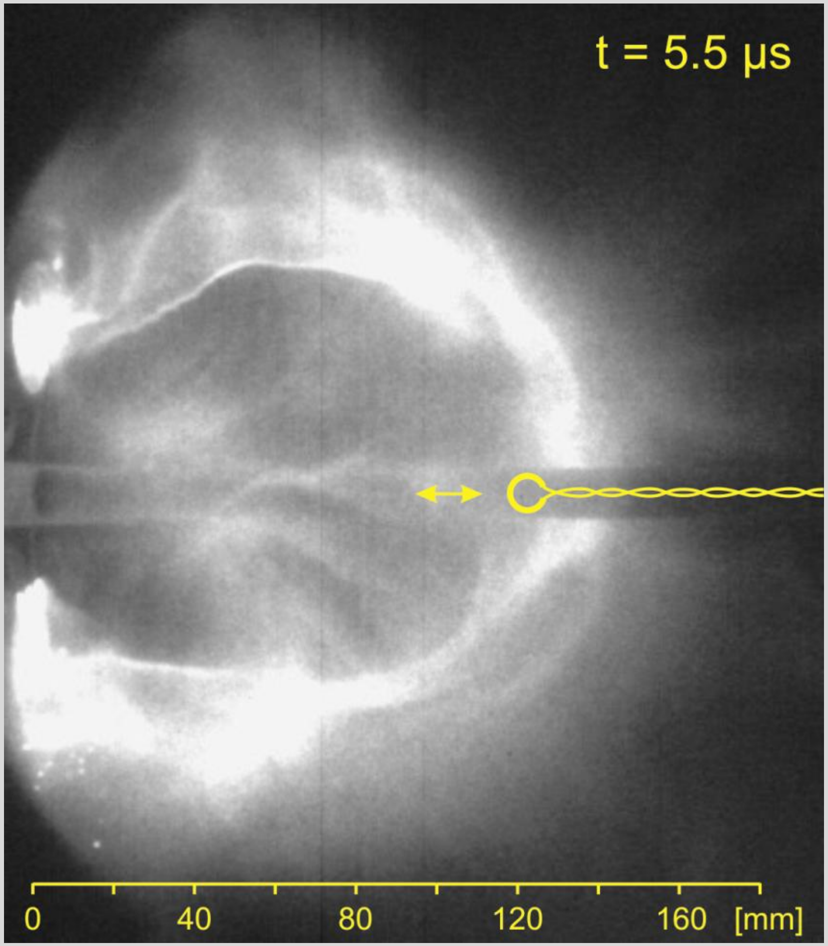

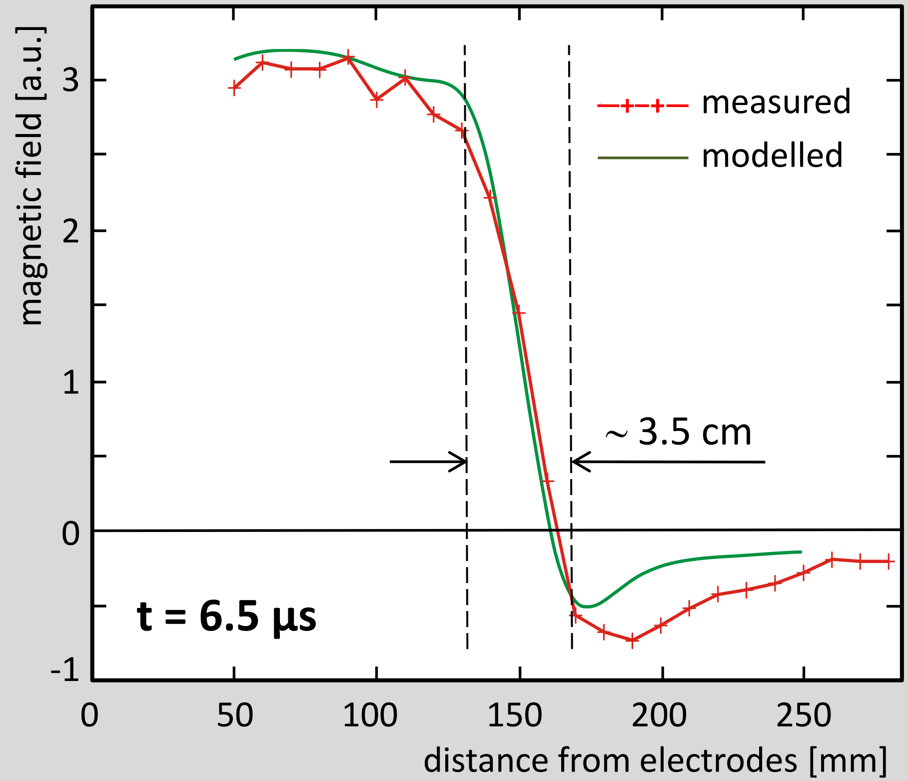

out-of-plane magnetic field component B_θ as a function of distance from electrodes

The FlareLab-Experiment: Measurement of plasma parameters (IV)

- **interferometer utilizing a CO_2 laser (λ = 9.4 µm)** $\rightarrow \int_L n_e \, ds$

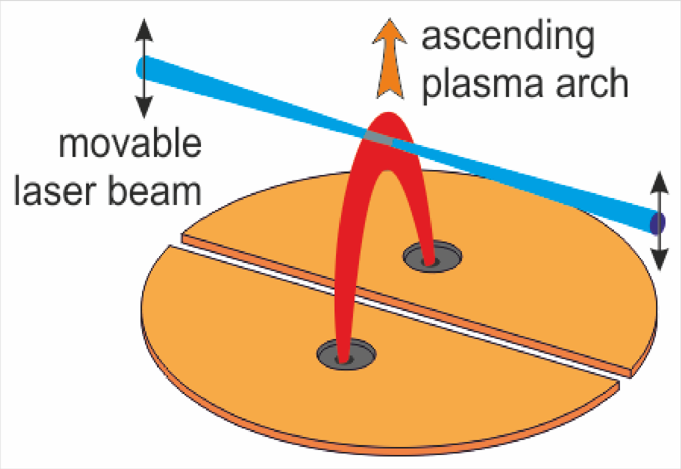

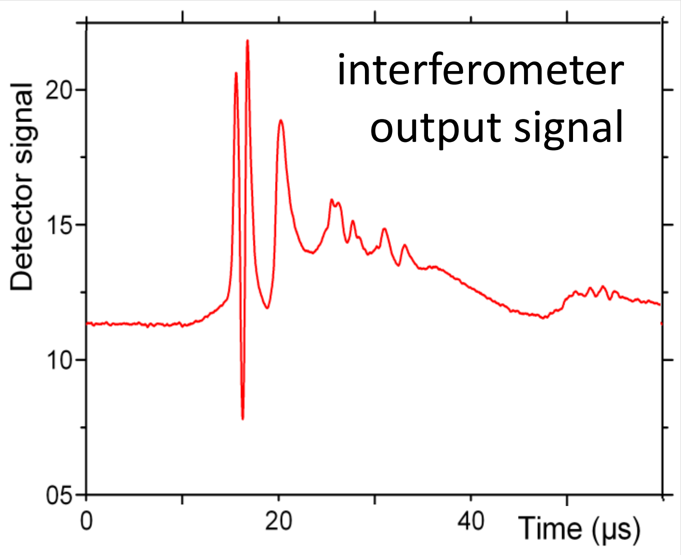

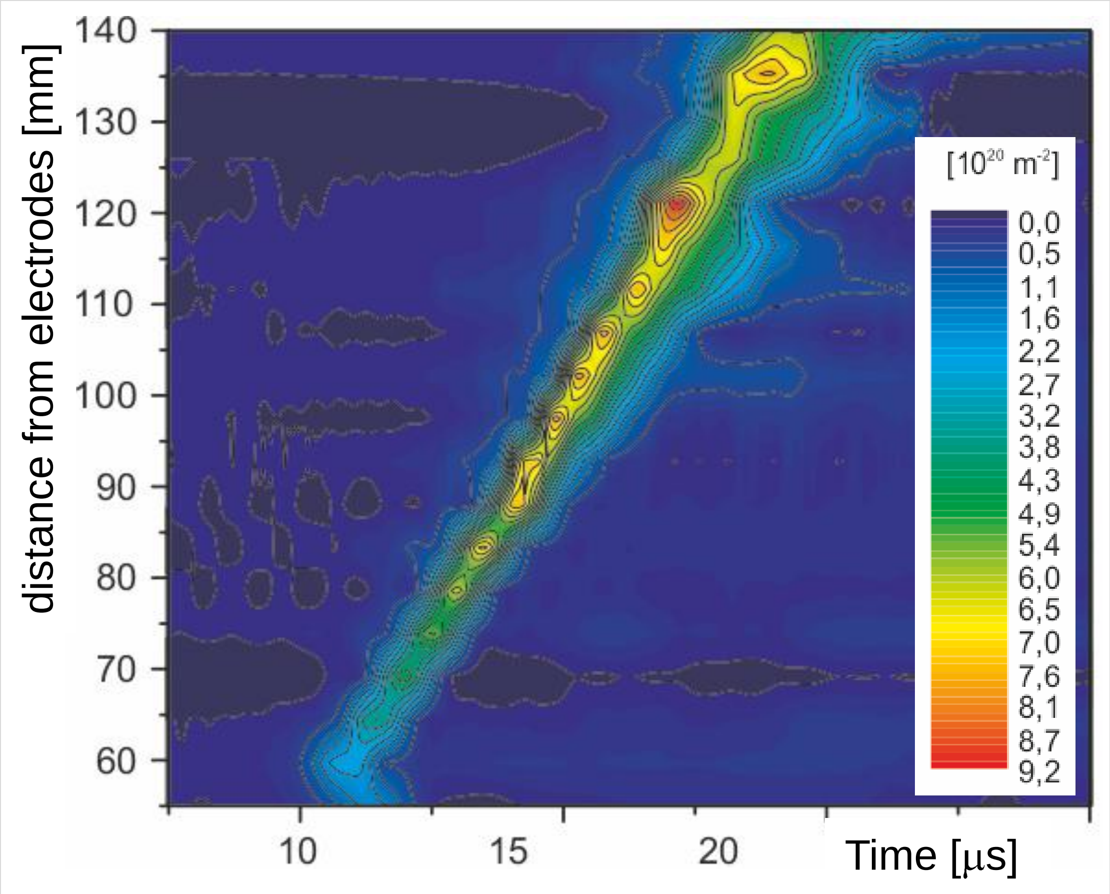

Phase shift in units of line-integrated electron density as a function of time and distance from the electrodes

The FlareLab-Experiment: Characteristic discharge parameters

RUB

plasma diameter	$d = 3\times10^{-2}$ m
plasma length	$L = 30\times10^{-2}$ m
electron density	$\overline{n}_e = 1\times10^{22}$ m^{-3}
electron temp.	$\overline{T}_e = 5$ eV
current density	$j = 2{,}8\times10^{7}$ A/m^2
magn. flux density	$B_p = 0.15$ T
rate of current rise	$dI/dt = 4$ kA/µs
injected gases	H_2, D_2, He, Ar

plasma beta:

$$\beta = \frac{n_e(T_e + T_i)}{B^2/2\mu_0} \approx 0.8$$

Lundquist number:

$$S = \mu_0 v_A \sigma \cdot L$$

$$\approx 190 \;\; (L = 0.3 \text{ m})$$

(res. skin time) : (plasma duration) $\tau_{res} : \tau_{exp} \cong 20\mu s : 8\mu s = 2.5$

Alfvén velocity $\cong$ **electron drift velocity** $\cong$ **expansion velocity** $\cong 2\times10^4$ m/s

ion Larmor radius $\rho_{ion} \cong 1.5$ mm ; **ion skin depth** $c/\omega_{pi} \cong 3$ mm

The FlareLab-Experiment: Evolution of flux tube morphology

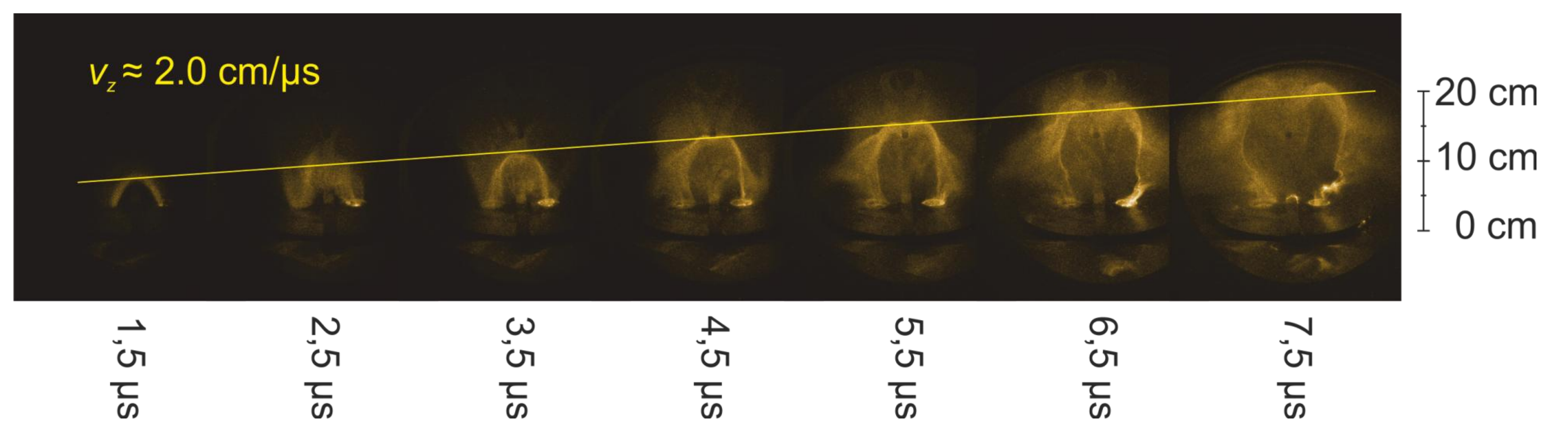

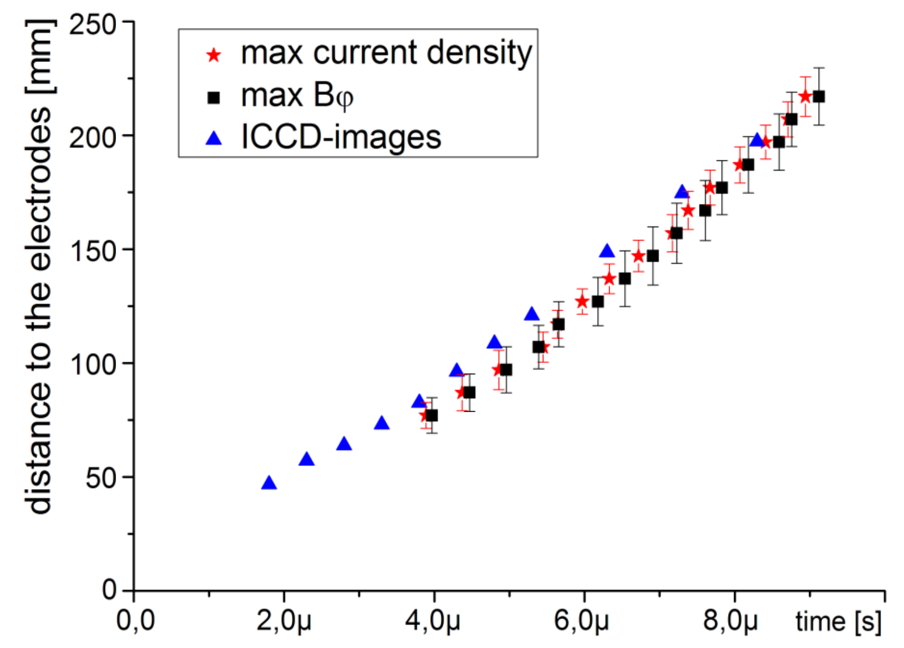

- **almost constant rate of ascend in the apex of the arch**
  (velocity depends on gas species and on the rate of current rise)
- **almost constant width of the current channel**
  (well-collimated flux tube with uniform cross section is formed shortly after gas breakdown)

The FlareLab-Experiment: Evidence of a MHD pumping mechanism?

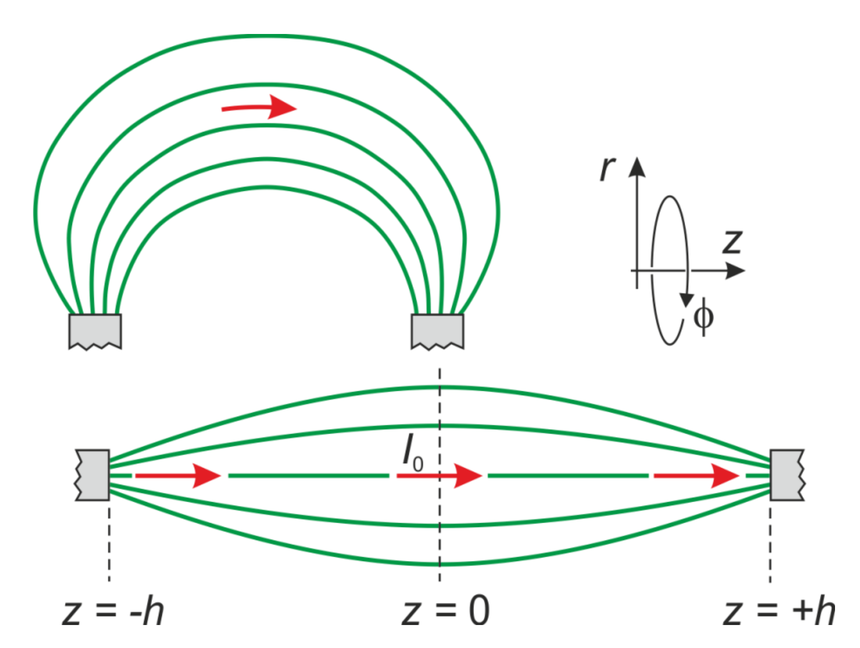

P. M. Bellan,
Why current-carrying magnetic flux tubes gobble up plasma and become thin as a result
Phys. Plasmas **10**, 1999 (2003)

→ flows from both foot points towards the center due to a total axial force:

$$F_z = (\mathbf{J} \times \mathbf{B})_z - \frac{\partial P}{\partial z} = \frac{\mu_0 I_0^2}{2\pi^2 a^3}\left(1 - \frac{r^2}{a^2}\right)\frac{\partial a}{\partial z}$$

Predictions:

- the mechanism causes a <u>strong increase of the plasma density</u> by ingesting particles from the electrode regions into the bulged flux tube;
- the ingested plasma convects frozen-in magnetic flux from $z = \pm h$ to $z = 0$, which increases the local azimuthal field B_ϕ and hence the pinch force, thus reducing the tube radius $a(0)$ and <u>forming a uniform cross-section</u>.

The FlareLab-Experiment: NO evidence of a MHD pumping mechanism

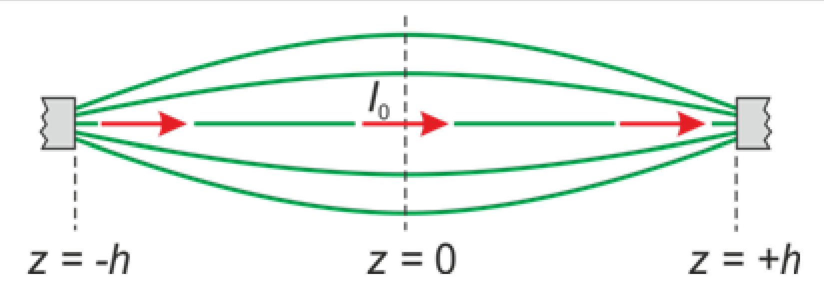

$$F_z = (\mathbf{J}\times\mathbf{B})_z - \frac{\partial P}{\partial z} = \frac{\mu_0 I_0^2}{2\pi^2 a^3}\left(1-\frac{r^2}{a^2}\right)\frac{\partial a}{\partial z}$$

$\frac{\partial a}{\partial z} = 0 \;\Rightarrow\; F_z = 0 \;\Rightarrow$ mechanism is not effective in a collimated flux tube

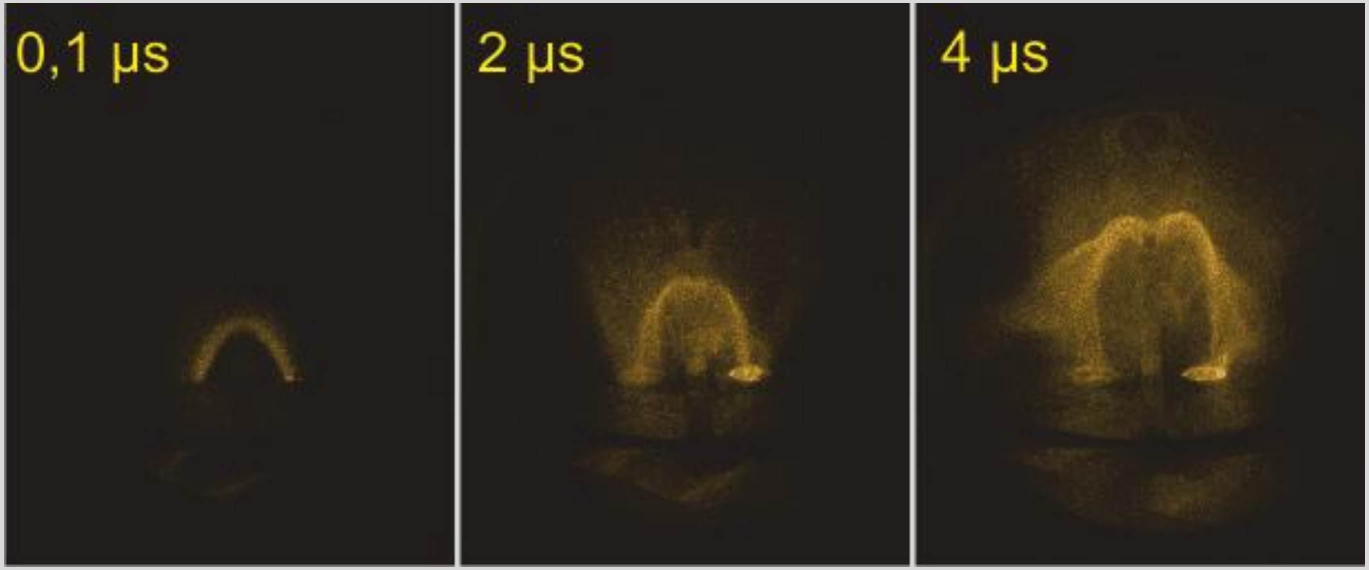

Initial discharge channel is thin and follows an arched path between the orifices in the electrodes;

discharge remains well collimated during expansion.

The FlareLab-Experiment: Plasma source without bulged magnetic field

original plasma source
(bulged dipole field lines)

↔

new line current source
(circular concentric field lines)

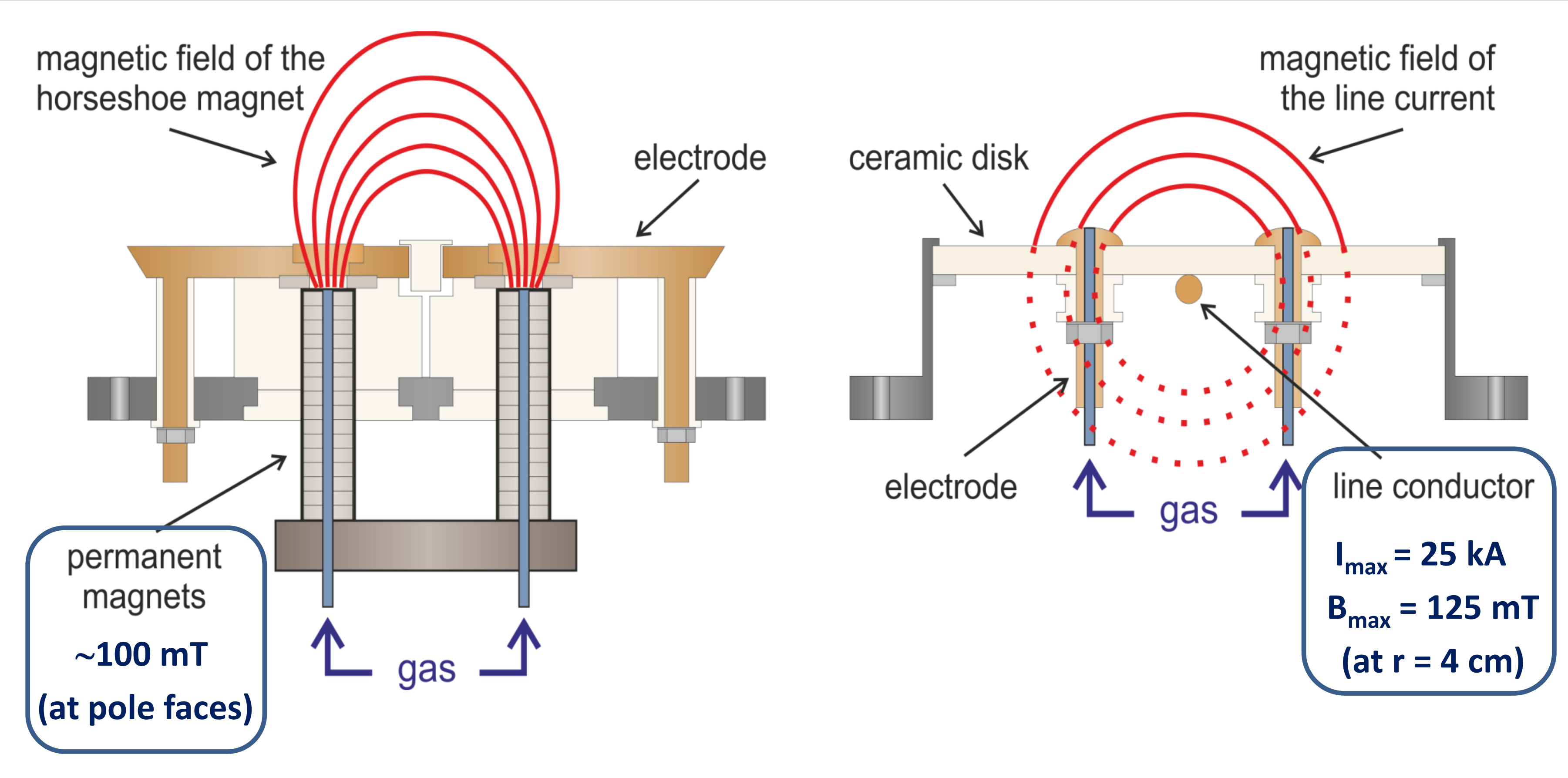

The FlareLab-Experiment: Evolution of flux tube morphology (new)

gas species: Argon; *line current*: 23 kA; *main capacitor bank*: ±3 kV

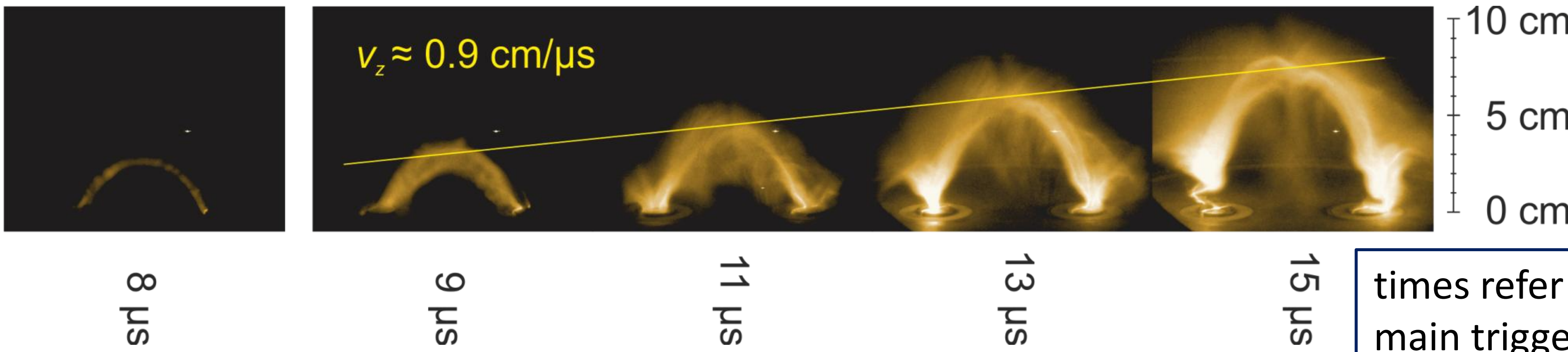

times refer to main trigger 8 μs before ignition.

- **smaller rate of ascend because of heavier gas**
  (Argon instead of Hydrogen-Helium mixtures as used in previous investigations)
- **general evolution of the discharge practically unchanged**
  (close similarity to the temporal development observed in the original setup including a kink-like deformation in the apex at a later time)
- **plasma density in the same order of magnitude as before**
  (neutral gas injection and discharge currents as before lead to comparable electron densities, although the proposed MHD pumping mechanism cannot be effective)

The FlareLab-Experiment: simple model to illustrate the loop expansion

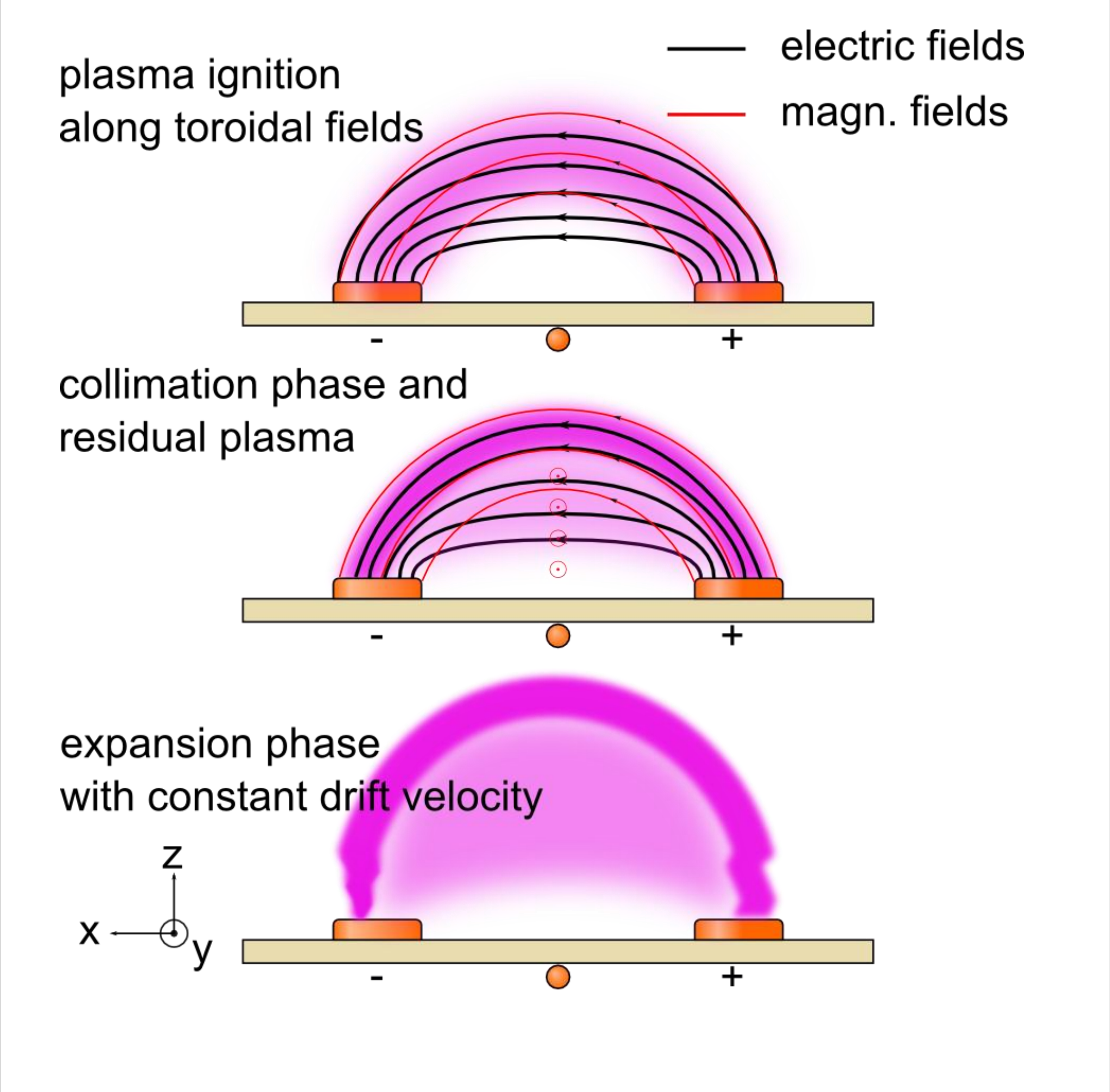

the **electric field** between electrodes and the poloidal **magnetic field** due to the plasma current are perpendicular to each other and cause an **E×B-drift** in upward direction.

The FlareLab-Experiment: Numerical simulation of arch expansion

first step: **Ideal MHD**

$$\frac{\partial \rho}{\partial t} = -\nabla \cdot (\rho \vec{v}) + S$$

$$\frac{\partial \vec{v}}{\partial t} = -(\vec{v} \cdot \nabla)\vec{v} + \frac{\vec{j} \times \vec{B}}{\rho} - \frac{\nabla p}{\rho} + \nu \Delta \vec{v}$$

$$\frac{\partial \vec{B}}{\partial t} = \nabla \times (\vec{v} \times \vec{B})$$

$$\nabla \times \vec{B} = \mu_0 \vec{j}$$

ρ : mass density

$\vec{v}$: bulk velocity

$\vec{B}$: magnetic field

p : thermal pressure

$\vec{j}$: current density

S : source term to implement different density models

$\nu \Delta \vec{v}$: viscosity term (formally included for numerical stability)

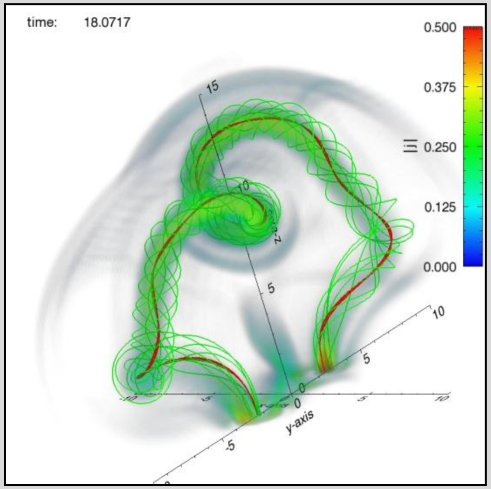

numerical implementation:
- finite differences on cartesian grid
- boundary condition in x-y-plane: $\vec{v} = 0$ ($\rightarrow$ line tying)
- adaptive mesh refinement

The FlareLab-Experiment: Numerical simulations (original source)

initial conditions for the magnetic field

a) field of horseshoe magnet

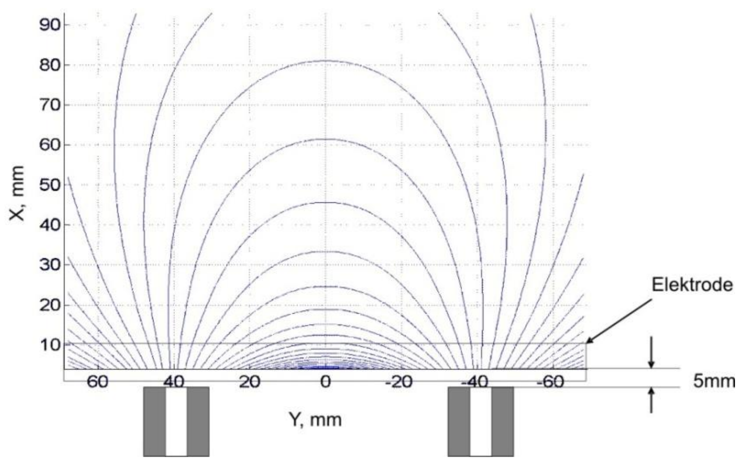

b) field of plasma current initially localized around semi-circle in the y-z-plane

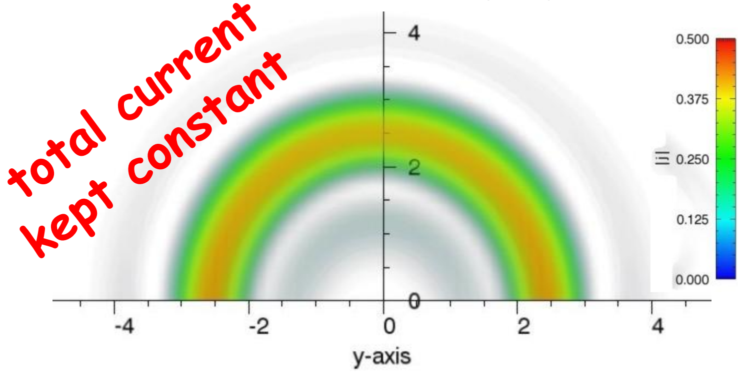

$$\frac{\partial \rho}{\partial t} = -\nabla \cdot (\rho \vec{v})$$

(mass conservation)

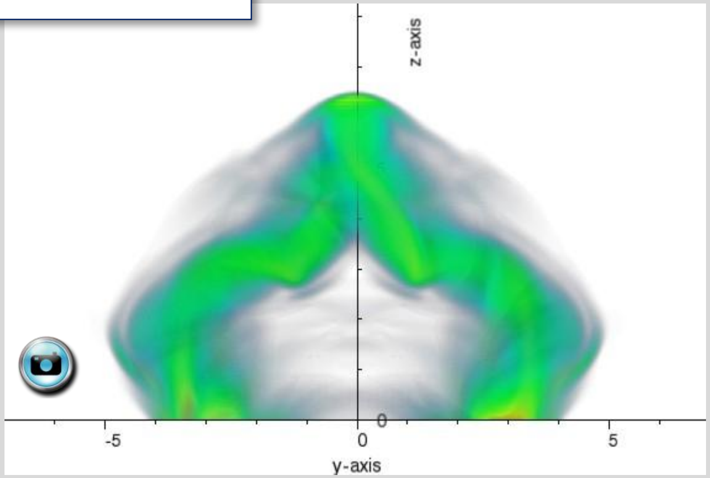

$$\rho(\vec{x}, t) = \frac{|\vec{B}(\vec{x}, t)|^2}{v_A^2}$$

(const. Alfvén velocity)

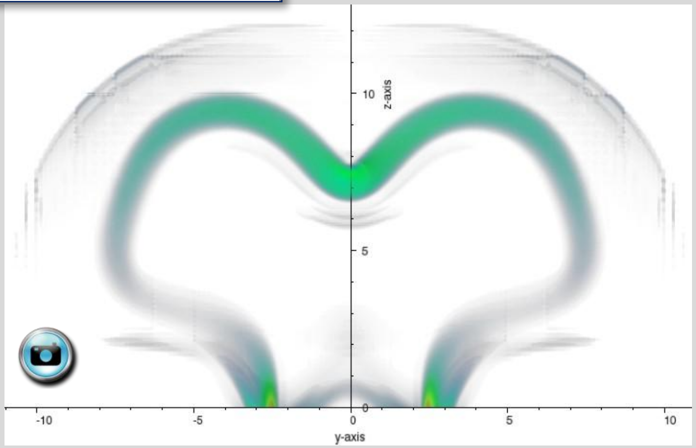

The FlareLab-Experiment: Numerical simulations (new source)

initial model configuration

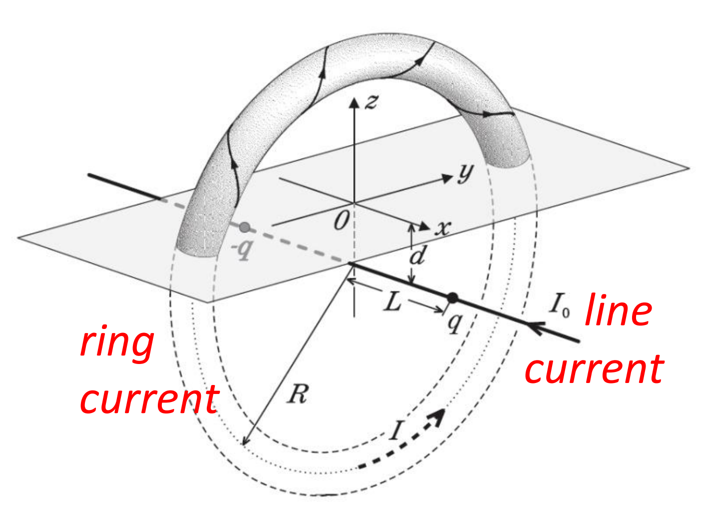

V.S. Titov and P. Démoulin,
Astron. Astrophys. **351**, 707 (1999)

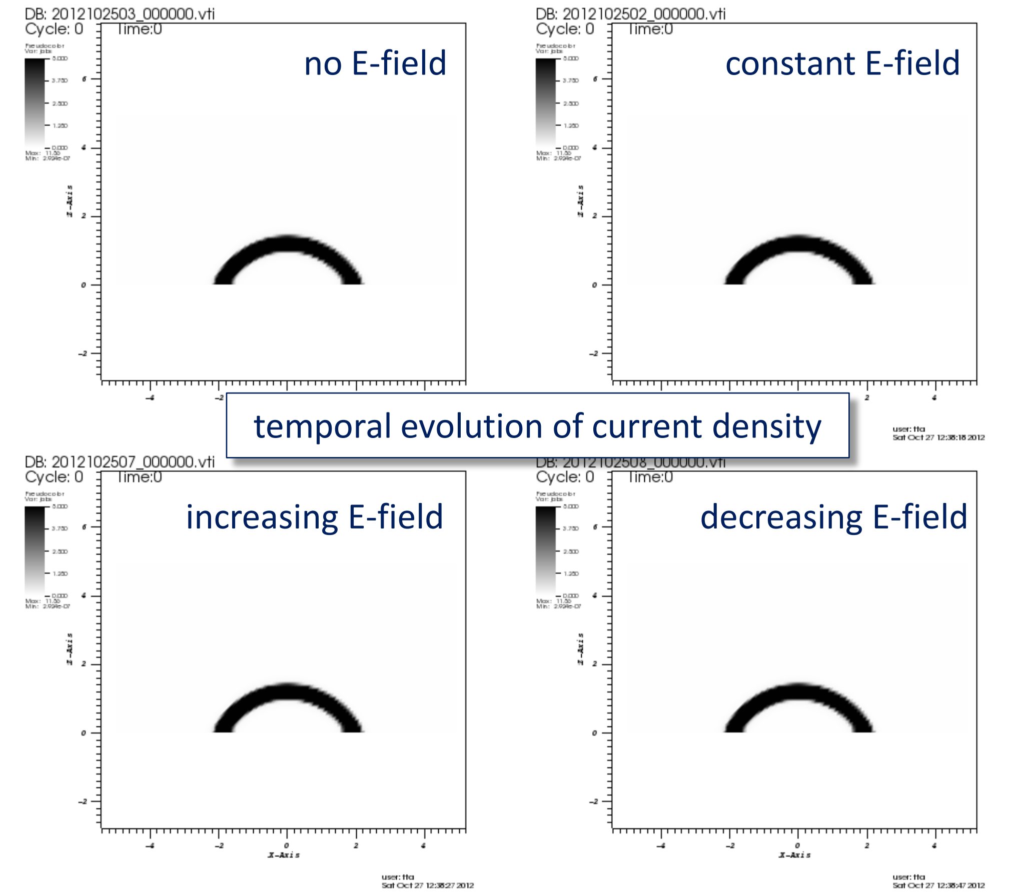

inclusion of finite resistivity
→ hinders the development of kinks

increase of the plasma current due to a prescribed E-field:

$$\mu_0 \frac{\partial}{\partial t} j_z = \frac{\partial}{\partial t} (\nabla \times \vec{B})_z = -(\nabla \times (\nabla \times \vec{E}))_z$$

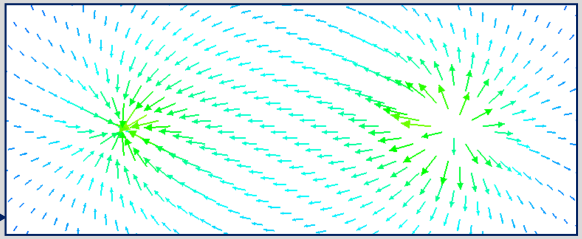

tangential E-field at lower boundary reflecting the applied voltage between electrodes

The FlareLab-Experiment: Numerical simulations (loop expansion)

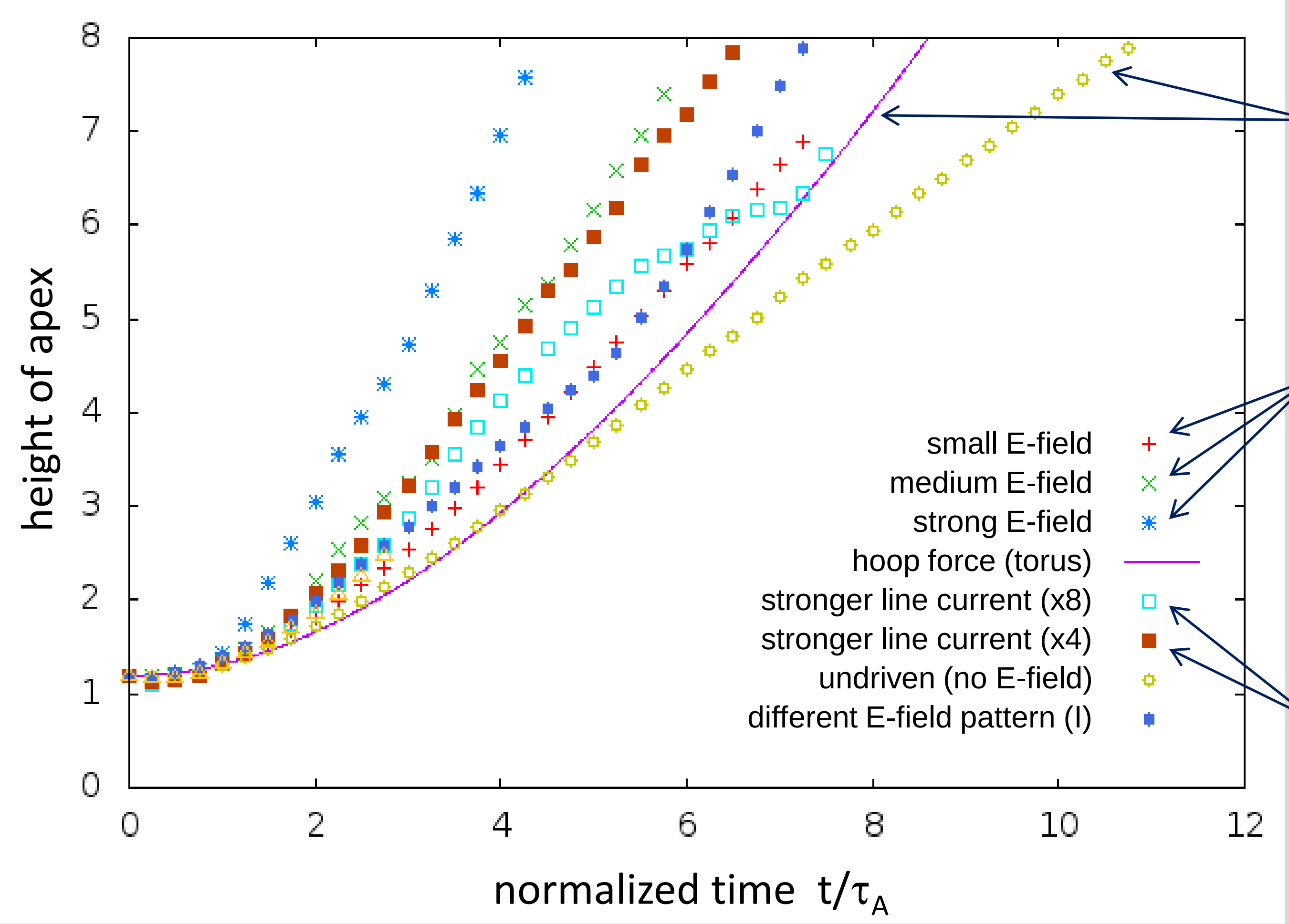

undriven case differs from toroidal hoop force expansion due to fixed foot points

driving enhances the rise velocity (as seen in the experiment)

stronger line current (= less twist) shows similar behavior, but reduces the outward bulges at the flanks and the small-scale kinking in the apex

- early phase dominated by acceleration and expansion due to magnetic hoop force
- later phase characterized by nearly constant expansion velocity under varying conditions

The FlareLab-Experiment: Current measurements (new source)

movable Rogowski coil (37 mm diameter) at various positions inside the vacuum vessel

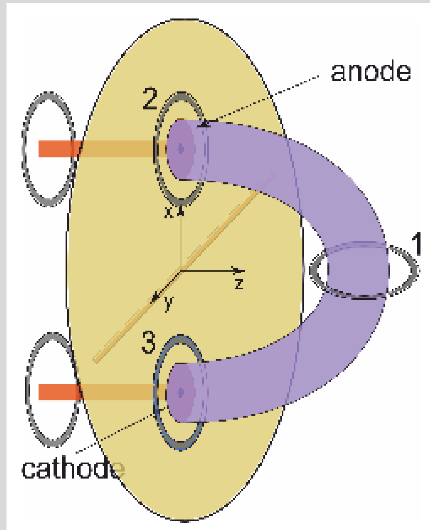

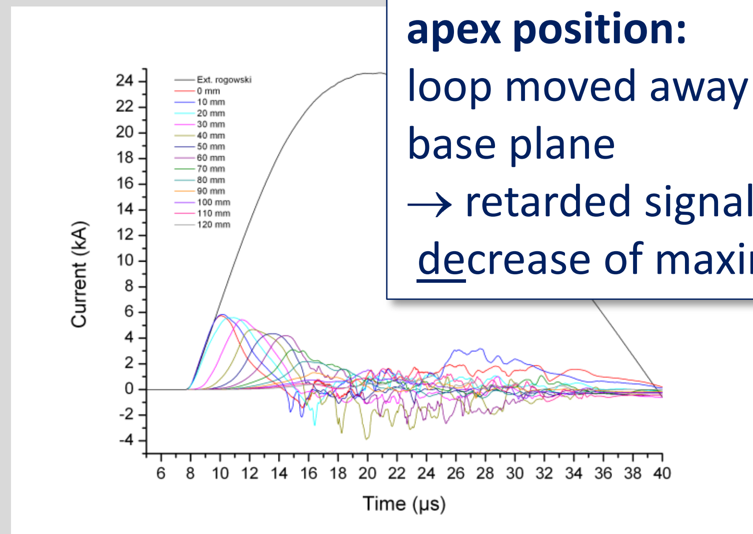

apex position:
loop moved away from base plane
→ retarded signal, but <u>de</u>crease of maximum

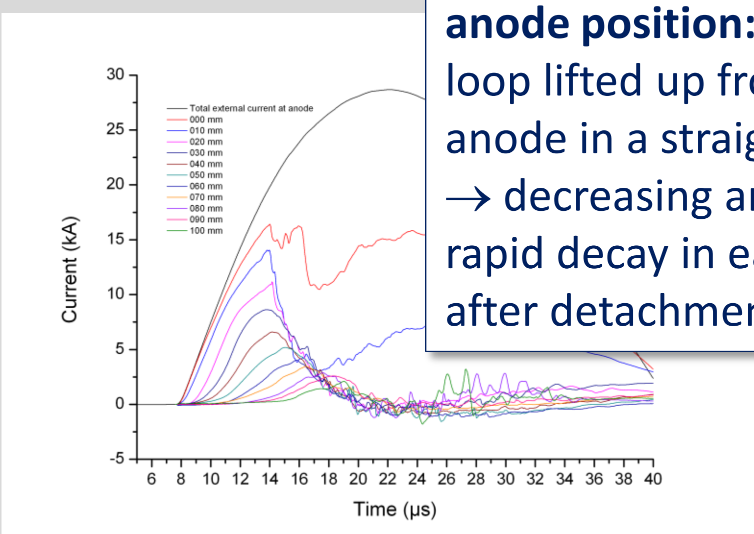

anode position:
loop lifted up from anode in a straight line
→ decreasing amplitude, rapid decay in each trace after detachment

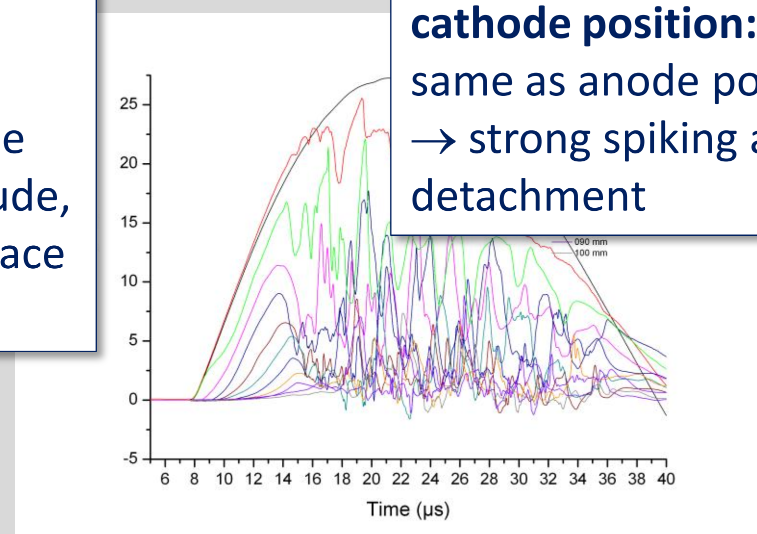

cathode position:
same as anode position
→ strong spiking after detachment

The FlareLab-Experiment: „Tornados“ and detachment from electrodes

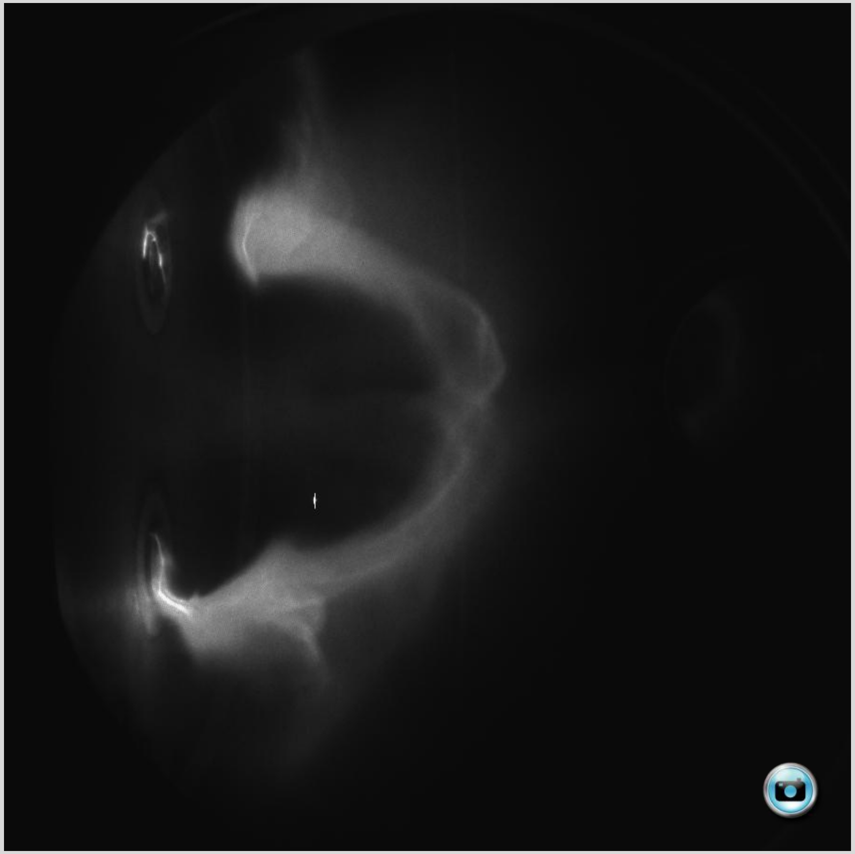

Discharge constricts and detaches from electrodes (starting at the anode); current continues to flow from the capacitor bank.

Contraction of the current channel at the electrodes and abrupt widening into a rather unshaped plasma bulk (similar to a tornado).

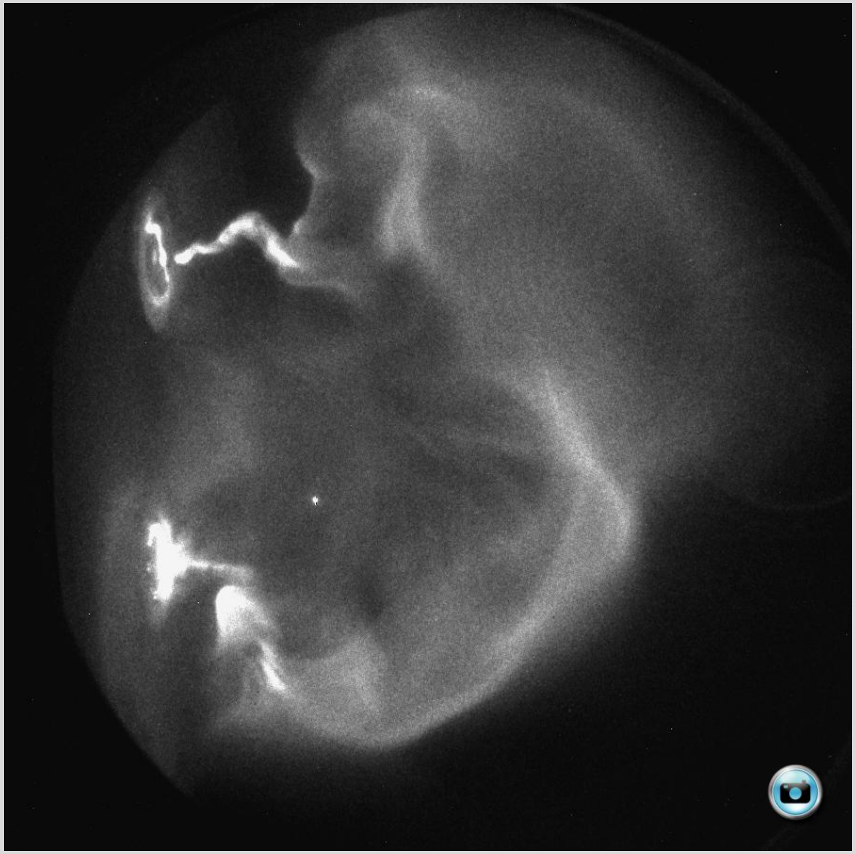

The FlareLab-Experiment: Numerical simulation of a „tornado“

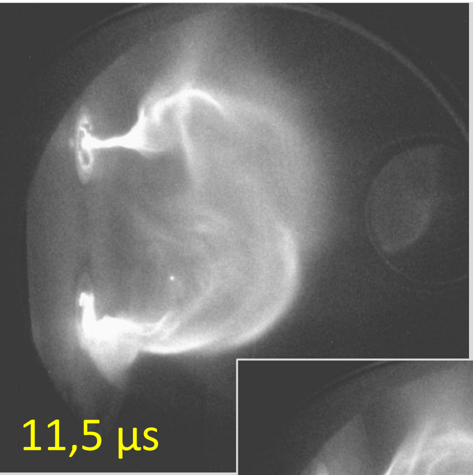

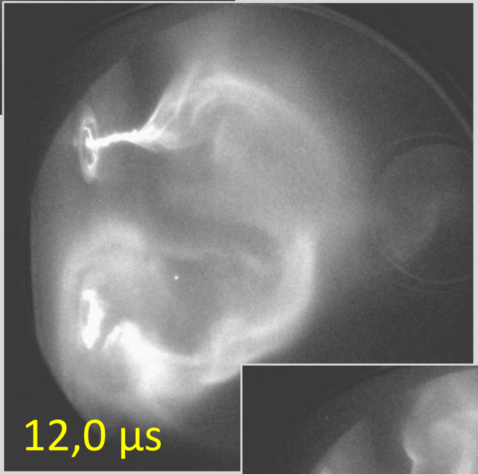

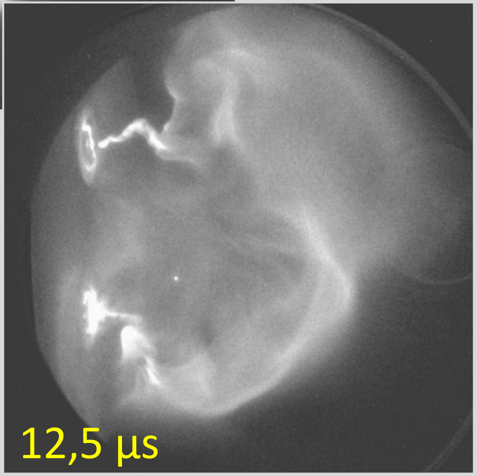

discharge in a He-H mixture; ±3 kV main bank; 24 kV aux. bank

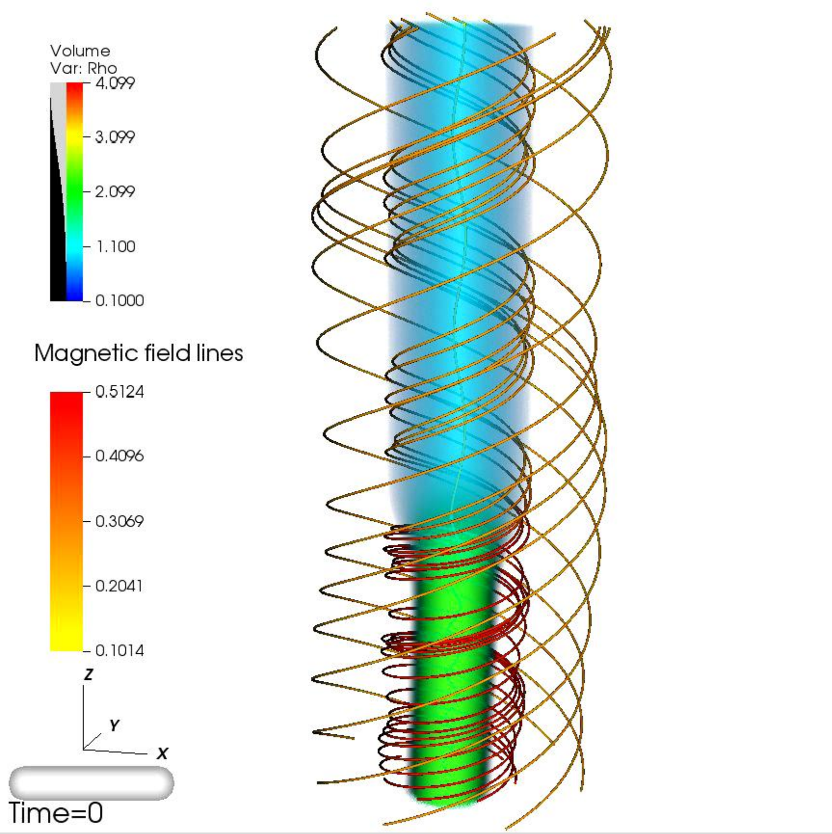

initial configuration is deformed and slightly widening in order to produce $j_r \times B_p$ force along the axis and to allow for growth of non-symmetric modes.

The FlareLab-Experiment: Further effects beyond simple ideal MHD

Weak magnetic guiding field:

appearance of persisting periodic structures within the arch-shaped plasma column and in its surroundings

0.3 µs after ignition

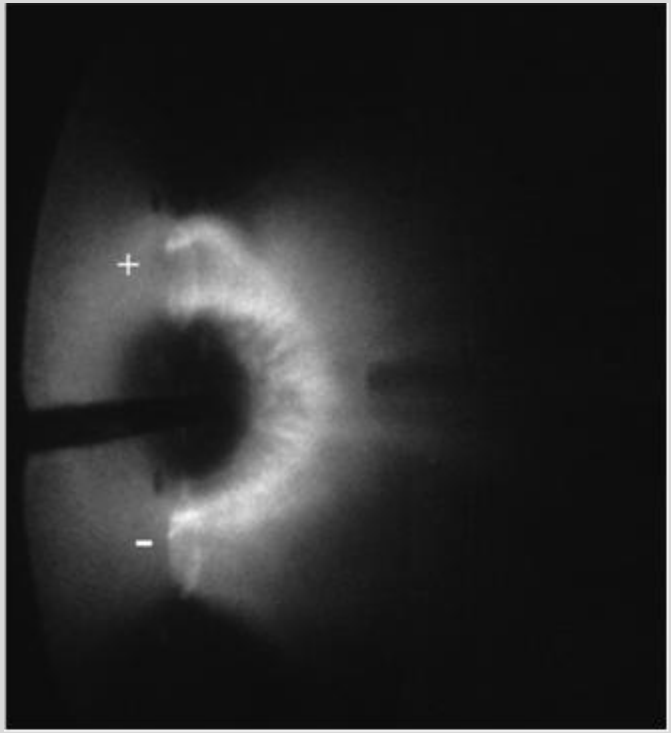

periodic modulation of luminosity inside the arch

0.9 µs after ignition

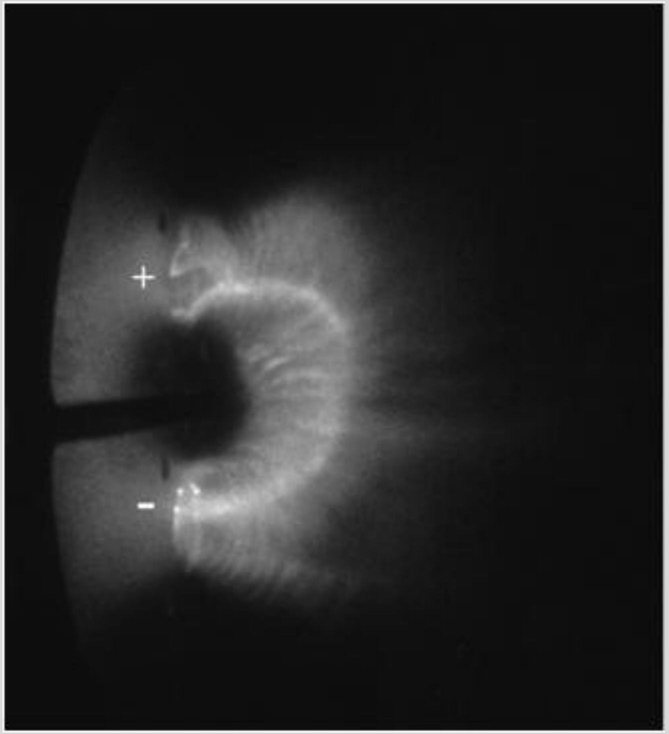

expansion of rib-like structure underneath the arch and appearance of ray-like tracers

→ Generation of fast particles ???

The FlareLab-Experiment: Detection of XUV radiation

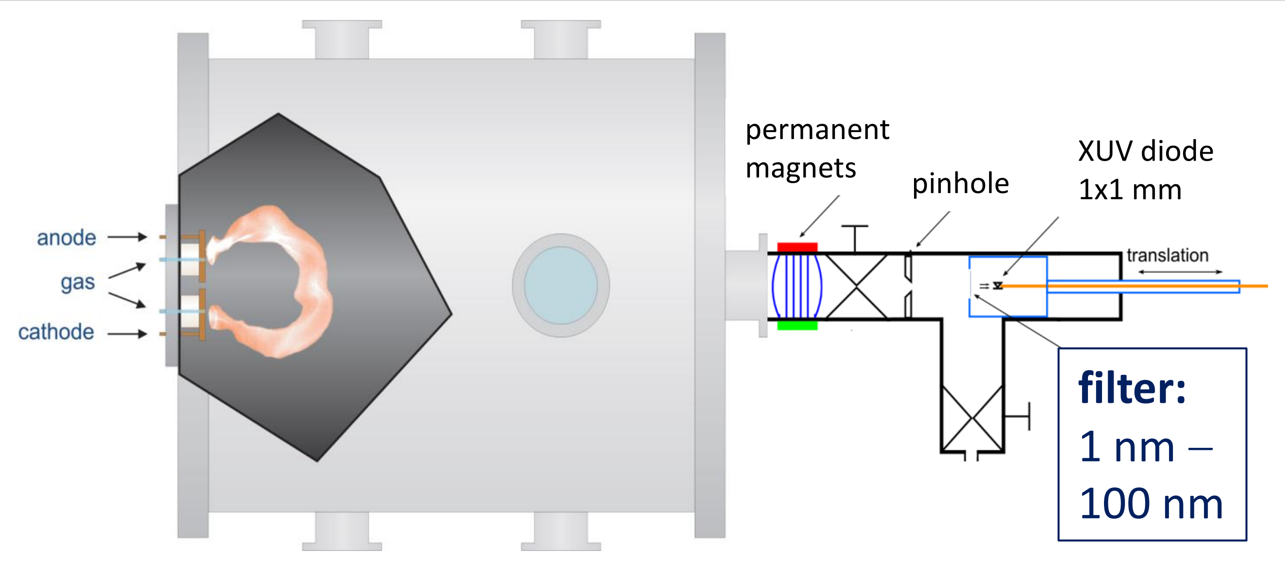

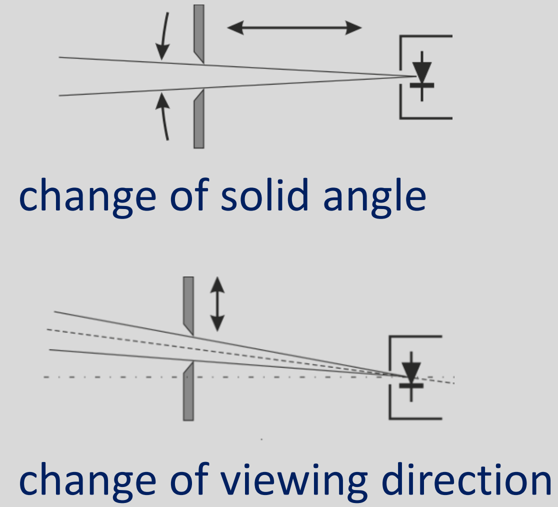

fast photodiode sensitive to visible and XUV radiation is installed at the back of the vessel;

permanent magnets in front of the pinhole deflect fast particles before they can reach the detector;

solid angle and viewing direction can be changed by means of a **movable pinhole**;

thin metal foils transmit energetic photons only.

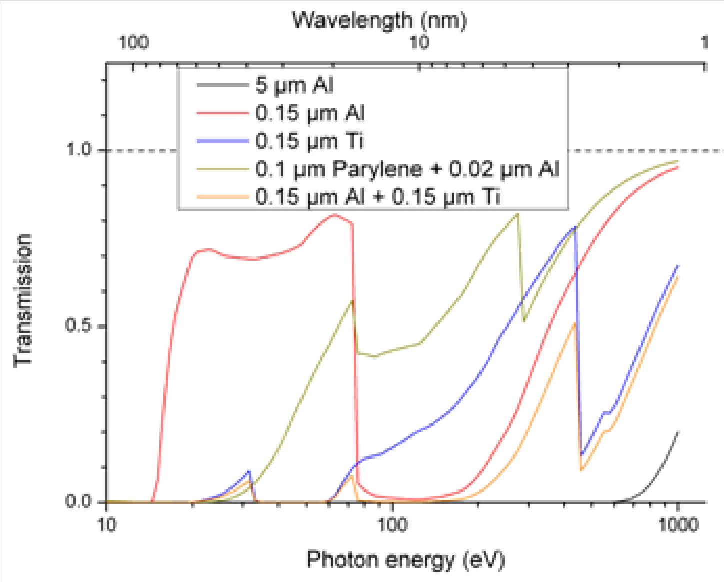

The FlareLab-Experiment: XUV radiation emitted from electrode regions

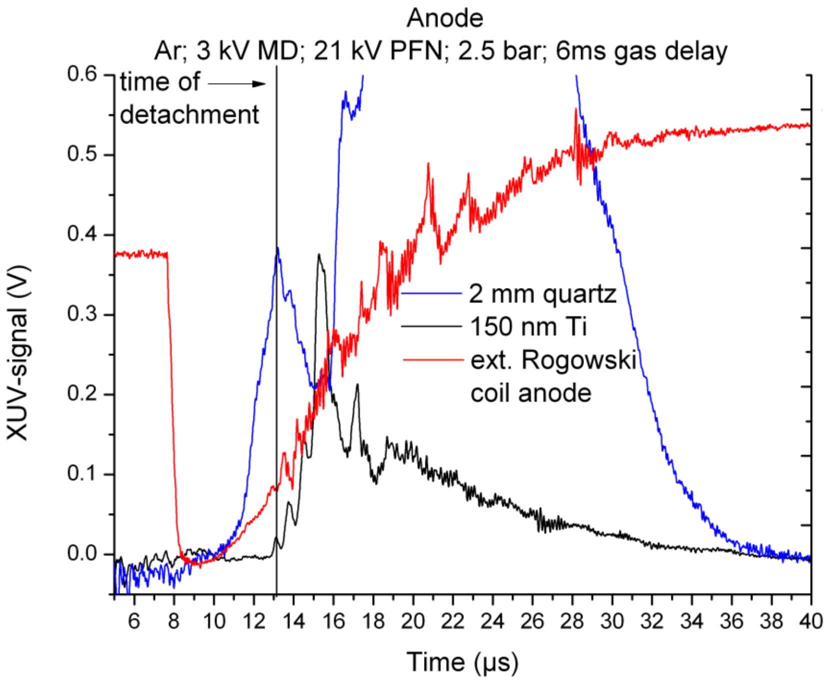

← Anode region

- visible light (blue curve)

decreases at time of detachment and increases strongly when XUV decays

- XUV light (>60 eV, black curve)

starts after detachment and decays fairly smoothly

Cathode region →

- visible light (blue curve)

decreases at time of detachment and decays fairly smoothly

- XUV light (>60 eV, black curve)

increases slowly after detachment and shows strong spiking afterwards

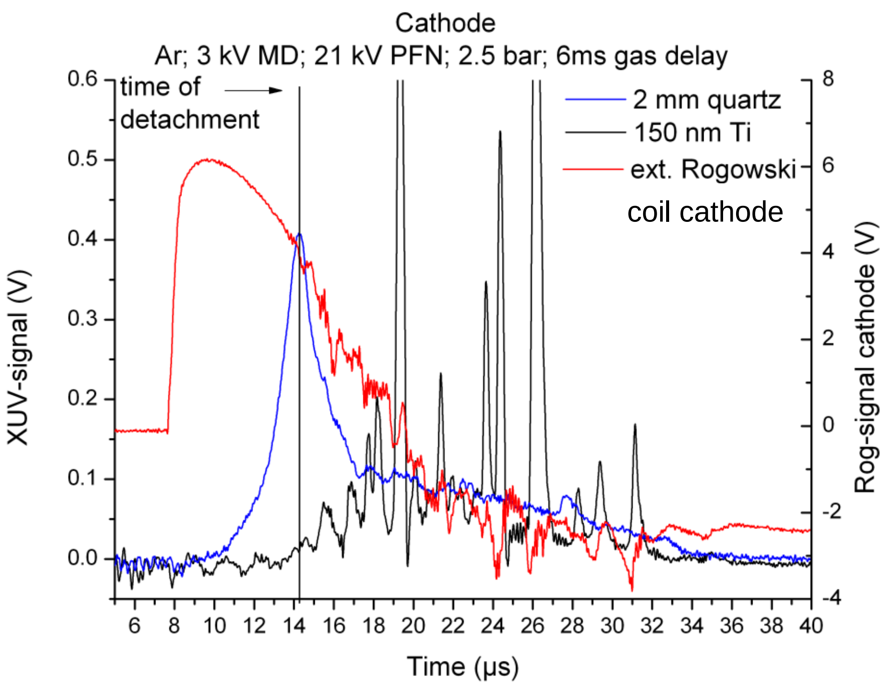

The FlareLab-Experiment: The Titov-Démoulin model

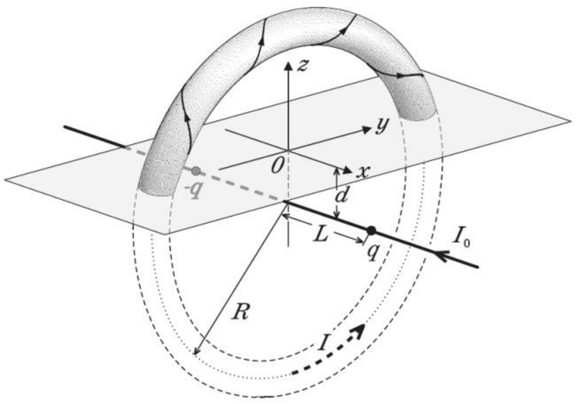

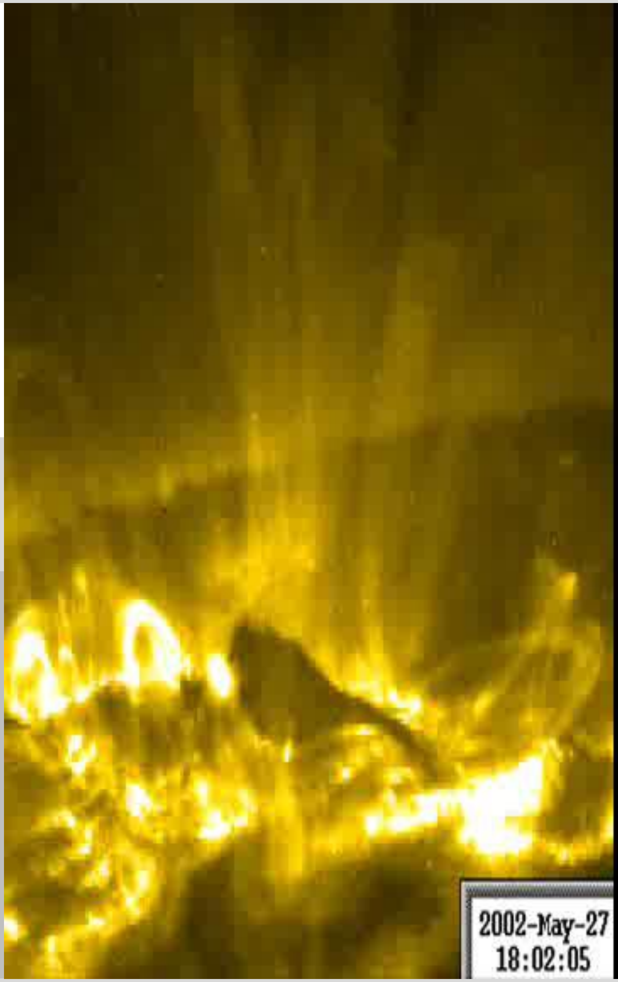

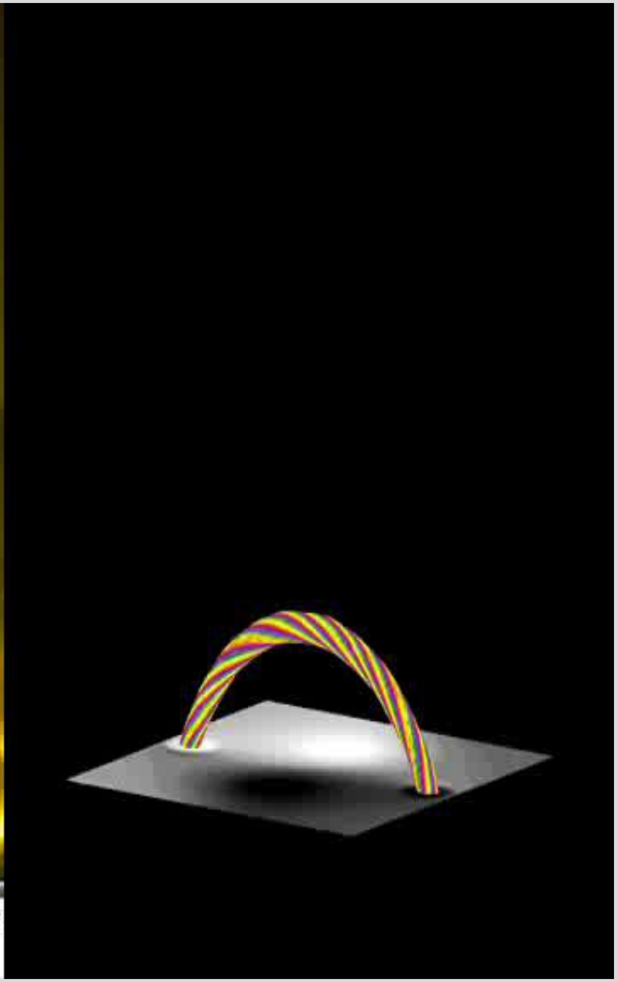

simulation by

T. Török and B.Kliem,

(Astrophys. Inst. Potsdam)

Astrophys. J. **630**,

L97-L100 (2005)

The FlareLab-Experiment: The Titov-Démoulin model

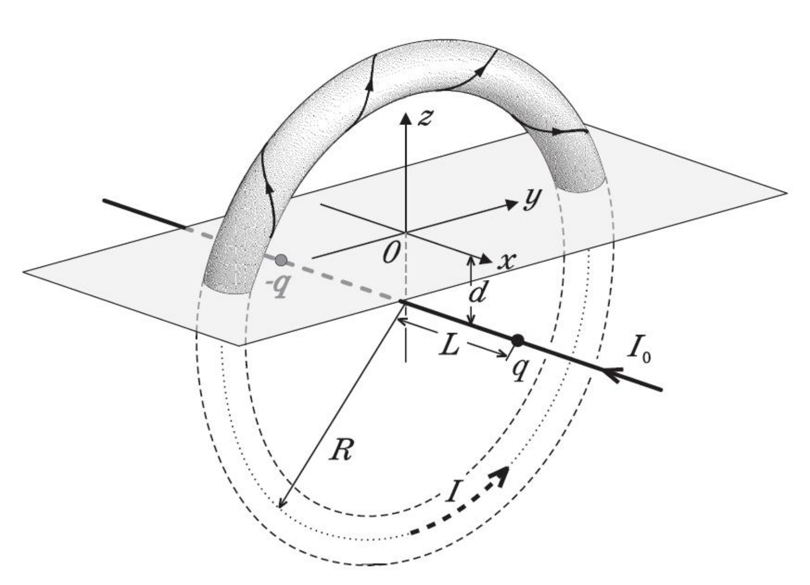

experimental realisation

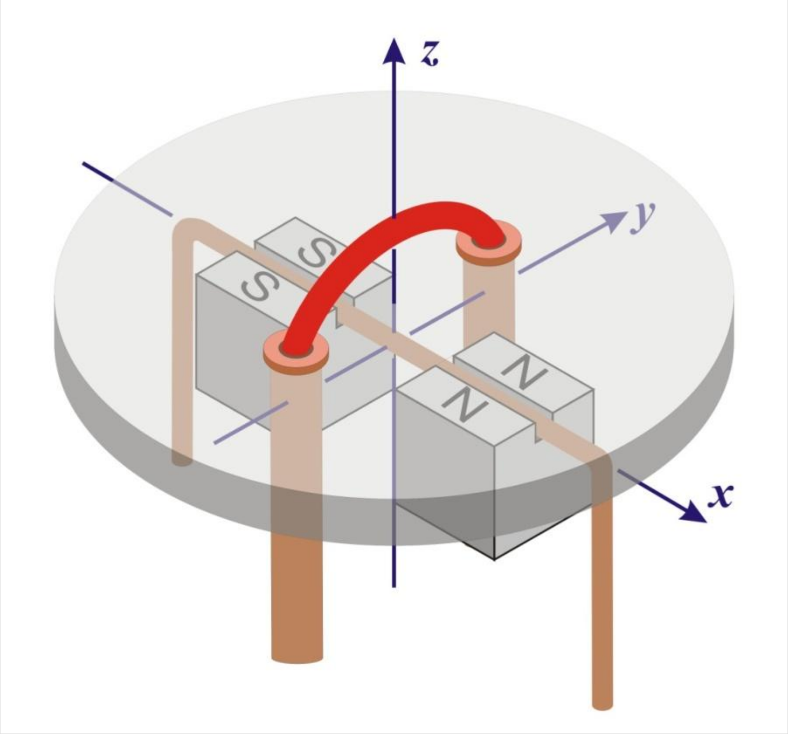

***q, -q* : „magnetic charges“** to produce dipole field

***I_0* :** line current to produce toroidal magnetic field

***I* :** ring current to produce poloidal magnetic field

The FlareLab-Experiment: Discharges with magnetic strapping field

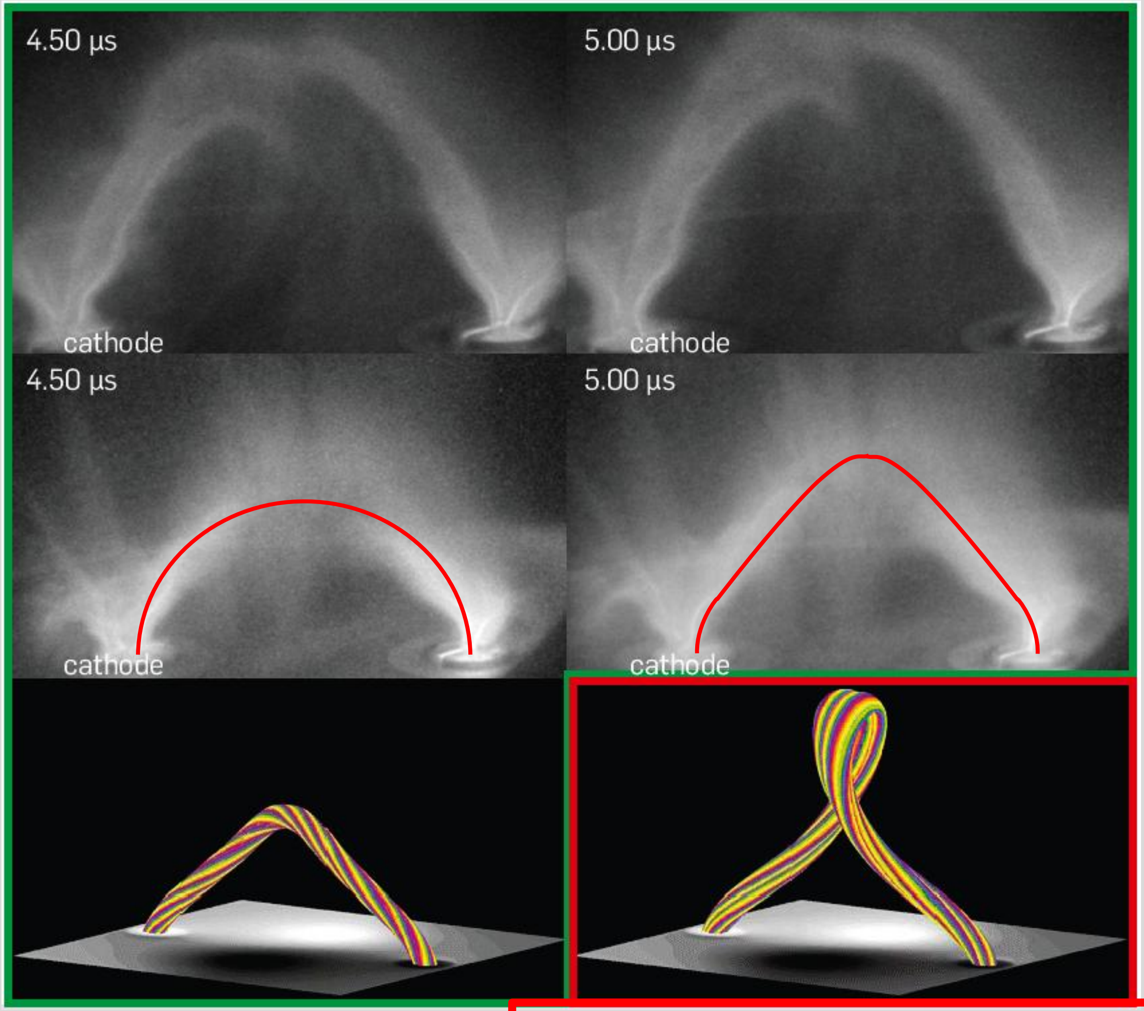

not yet observed in experiment

without strapping field

plasma shows a relatively fast and uniform expansion

with strapping field

- flux tube expands more slowly,
- shape of flux tube evolves from semi-circular to triangular.

simulation by Török and Kliem

starting from a semi-circular configuration, the flux tube attains a triangular shape and develops a strong outward twist.

The FlareLab-Experiment: Summary

reliable and fairly reproducible plasma production for different configurations and operational conditions:

- high degree of ionization, but rather resistive;
- prone to macroscopic and small-scale instabilities;
- generation of fast particles (and energetic photons);
- phenomena near electrodes (“tornados”, detachment)

P.M. Bellan & J.F. Hansen, Proc. of ISSS-6, 192 (2001)

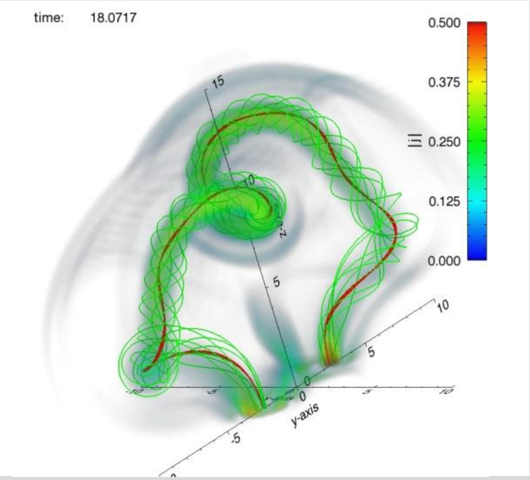

L. Arnold, J. Dreher et al., Phys. Plasmas **15**, 042106 (2008)

extensive time-dependent 3-dimensional MHD calculations using adaptive mesh refinement:

- arch expansion for different density models;
- arch expansion using special drivers for $\Delta I_p > 0$;
- development of kink modes;
- simulation of “tornados” and detachment.